



THE UNIVERSITY *of* EDINBURGH

Edinburgh Research Explorer

Measurement of the W^+W^- production cross section in pp collisions at a centre-of-mass energy of $\sqrt{s} = 13$ TeV with the ATLAS experiment

Citation for published version:

Clark, PJ, Leonidopoulos, C, Martin, VJ, Mills, C, Collaboration, A, Mijovic, L, Gao, Y & Farrington, S 2017, 'Measurement of the W^+W^- production cross section in pp collisions at a centre-of-mass energy of $\sqrt{s} = 13$ TeV with the ATLAS experiment', *Physics Letters B*, vol. B773, Aaboud:2017qkn, pp. 354-374. <https://doi.org/10.1016/j.physletb.2017.08.047>

Digital Object Identifier (DOI):

[10.1016/j.physletb.2017.08.047](https://doi.org/10.1016/j.physletb.2017.08.047)

Link:

[Link to publication record in Edinburgh Research Explorer](#)

Document Version:

Publisher's PDF, also known as Version of record

Published In:

Physics Letters B

General rights

Copyright for the publications made accessible via the Edinburgh Research Explorer is retained by the author(s) and / or other copyright owners and it is a condition of accessing these publications that users recognise and abide by the legal requirements associated with these rights.

Take down policy

The University of Edinburgh has made every reasonable effort to ensure that Edinburgh Research Explorer content complies with UK legislation. If you believe that the public display of this file breaches copyright please contact openaccess@ed.ac.uk providing details, and we will remove access to the work immediately and investigate your claim.





Measurement of the W^+W^- production cross section in pp collisions at a centre-of-mass energy of $\sqrt{s} = 13$ TeV with the ATLAS experiment



The ATLAS Collaboration*

ARTICLE INFO

Article history:

Received 16 February 2017

Received in revised form 2 June 2017

Accepted 21 August 2017

Available online 30 August 2017

Editor: M. Doser

ABSTRACT

The production of opposite-charge W -boson pairs in proton–proton collisions at $\sqrt{s} = 13$ TeV is measured using data corresponding to 3.16 fb^{-1} of integrated luminosity collected by the ATLAS detector at the CERN Large Hadron Collider in 2015. Candidate W -boson pairs are selected by identifying their leptonic decays into an electron, a muon and neutrinos. Events with reconstructed jets are not included in the candidate event sample. The cross-section measurement is performed in a fiducial phase space close to the experimental acceptance and is compared to theoretical predictions. Agreement is found between the measurement and the most accurate calculations available.

© 2017 The Author. Published by Elsevier B.V. This is an open access article under the CC BY license (<http://creativecommons.org/licenses/by/4.0/>). Funded by SCOAP³.

1. Introduction

The measurement of the production properties of opposite-charge W -boson pairs (denoted by WW in this Letter) is an important test of the Standard Model (SM) of particle physics. This process is sensitive to the strong interaction between quarks and gluons and probes the electroweak gauge structure of the SM.

Measurements of WW production were first conducted at LEP [1] using electron–positron collisions. Measurements in hadron collisions were first carried out at the Tevatron by the CDF [2,3] and DØ [4] Collaborations. At the Large Hadron Collider (LHC), the WW production cross sections have been measured in proton–proton collisions for centre-of-mass energies of $\sqrt{s} = 7$ TeV and $\sqrt{s} = 8$ TeV by the ATLAS [5,6] and CMS [7,8] Collaborations. In order to match the experimental precision and address discrepancies between data and theory reported in some of the 8 TeV results, significant progress has been made in theoretical calculations to include higher-order corrections in perturbative Quantum Chromodynamics (pQCD) [9–14]. The WW signal is composed of three leading sub-processes: $q\bar{q} \rightarrow WW$ production¹ (in the t - and s -channels), non-resonant $gg \rightarrow WW$ production, and resonant $gg \rightarrow H \rightarrow WW$ production (with both gg -initiated processes occurring through a quark loop). These sub-processes are known theoretically at different orders in the strong coupling constant α_s .

This Letter describes a measurement of WW production in proton–proton collisions at $\sqrt{s} = 13$ TeV with the ATLAS detector using the data collected during the 2015 run. The cross sec-

tion is measured within a phase space close to the geometric and kinematic acceptance of the experimental analysis, i.e. a fiducial phase space, in the $WW \rightarrow e^\pm \nu \mu^\mp \nu$ (denoted in the following by $WW \rightarrow e\mu$) decay channel. In addition, the ratio of cross sections at 13 TeV and 8 TeV centre-of-mass energies in the respective fiducial phase spaces is presented. Both measurements are compared to the latest theoretical predictions.

2. The ATLAS detector

The ATLAS detector [15,16] is a multi-purpose particle detector with a cylindrical geometry.² It consists of layers of inner tracking detectors surrounded by a superconducting solenoid, calorimeters, and a muon spectrometer. The inner detector (ID) is situated inside a 2 T magnetic field generated by the solenoid and provides precision tracking for charged particles with pseudorapidity $|\eta| < 2.5$. The calorimeter covers the pseudorapidity range $|\eta| < 4.9$. Within $|\eta| < 2.47$ the finely segmented electromagnetic calorimeter identifies electromagnetic showers and measures their energy and position, providing electron identification together with the ID. The muon spectrometer (MS) surrounds the calorimeters and includes three large air-core toroidal superconducting magnets with eight

² The ATLAS experiment uses a right-handed coordinate system with its origin at the nominal pp interaction point at the centre of the detector. The positive x -axis is defined by the direction from the interaction point towards the centre of the LHC ring, with the positive y -axis pointing upwards, while the beam direction is along the z -axis. Cylindrical coordinates (r, ϕ) are used in the transverse (x, y) plane, ϕ being the azimuthal angle around the beam direction. The pseudorapidity is defined in terms of the polar angle θ from the z -axis as $\eta = -\ln[\tan(\theta/2)]$. The distance in η - ϕ space between two objects is defined as $\Delta R \equiv \sqrt{(\Delta\eta)^2 + (\Delta\phi)^2}$. Transverse energy is computed as $E_T = E \cdot \sin \theta$.

* E-mail address: atlas.publications@cern.ch.

¹ In this Letter, the notation $q\bar{q} \rightarrow WW$ is used to include both the $q\bar{q}$ and qg initial states for WW production.

coils each, providing muon identification and measurement in the region $|\eta| < 2.7$ and triggering in the region $|\eta| < 2.4$. A two-level trigger system is used to select events in real time. It consists of a hardware-based first-level trigger and a software-based high-level trigger. The latter uses reconstruction software with algorithms similar to the offline versions.

3. Data and Monte Carlo samples

The analysis is based on data collected with the ATLAS detector during the 2015 data-taking period. Events with pp collisions at $\sqrt{s} = 13$ TeV and all relevant detector components functional have been used. This data sample corresponds to an integrated luminosity of $\mathcal{L} = 3.16 \text{ fb}^{-1}$.

Monte Carlo (MC) event generators are used to model signal and background processes. The WW , WZ , and ZZ diboson processes (where Z stands for Z/γ^*) with $q\bar{q}$ initial states are simulated at next-to-leading order (NLO) in pQCD with the POWHEG-BOX v2 event generator [17–21] using the CT10 NLO [22] parton distribution functions (PDFs). For the modelling of the parton shower and non-perturbative effects such as fragmentation and the underlying event, POWHEG-BOX v2 is interfaced to PYTHIA v8.210 [23] with the AZNLO [24] set of tuned parameters and the CTEQ6L1 [25] PDF. The invariant mass of the leptons originating from the Z boson or photon in the ZZ and WZ samples is required to satisfy $m_{\ell\ell} > 7$ GeV. A sample of WZ events generated with SHERPA v2.1.1 [26] with $m_{\ell\ell} > 0.45$ GeV is used to study systematic uncertainties. The cross sections given by the event generator are at NLO in QCD while the WW , WZ and ZZ samples are normalised using their respective inclusive next-to-next-to-leading order (NNLO) predicted cross sections [9,27–29]. The configuration of the POWHEG-BOX v2 event generator, as described above, reproduces the distribution predicted by NNLO calculations matched to resummation calculations up to next-to-next-to-leading logarithm (NNLL) [9,10] for the transverse momentum of the WW system (p_T^{WW}) in the range relevant to this analysis, so no further steps are taken to explicitly include resummation effects in the WW signal samples. The resonant $gg \rightarrow H \rightarrow WW$ signal contribution is simulated with the POWHEG-BOX v2 event generator [30] and normalised using the inclusive next-to-next-to-next-to-leading order (N^3 LO) predicted cross section [31]. The non-resonant $gg \rightarrow WW$ signal contribution is modelled with SHERPA v2.1.1 at leading order (LO) using OpenLoops with up to one additional parton in the final state [32] and normalised using the inclusive NLO predicted cross section [33].

The $Z(\rightarrow e\bar{e}/\mu\bar{\mu}/\tau\bar{\tau}) + \text{jets}$ production processes are simulated with the Madgraph5_aMC@NLO v2.2.2 [34] event generator interfaced to Pythia v8.186. The matrix elements for Z production with up to four associated partons are calculated at LO and the NNPDF2.3 LO PDF set [35] is used. The PHOTOS++ program version 3.52 [36] is used for QED emissions from electroweak vertices and charged leptons. Alternative samples of $Z(\rightarrow \tau\bar{\tau}) + \text{jets}$ are produced with different MC event generators for the estimation of systematic uncertainties in the modelling: POWHEG-BOX v2 with NLO matrix elements interfaced to PYTHIA v8.210, and SHERPA v2.2.0 with NLO matrix-element accuracy up to two associated partons and with LO accuracy for three and four associated partons. The $Z + \text{jets}$ events are normalised using the NNLO Z production cross section [37].

The SHERPA v2.1.1 event generator is used to model the $W\gamma$ and $Z\gamma$ processes with LO matrix element calculations for events with up to 3 partons in the final state matched to parton shower, using the CT10 NLO PDF set and with the γ transverse momentum greater than 10 GeV.

The POWHEG-BOX v2 event generator [38,39] with the CT10 NLO PDF is used for the generation of $t\bar{t}$ and single top quarks in the Wt channel. Parton shower, fragmentation, and the underlying event are simulated using PYTHIA v6.428 [40] with the CTEQ6L1 PDF and the Perugia 2012 [41] set of parameters. The top-quark mass is set to 172.5 GeV. Alternative samples are generated with different settings to assess the uncertainty in modelling top-quark events. For estimating the effect of parton shower and hadronisation modelling an alternative sample is generated with the POWHEG-BOX v2 event generator interfaced to HERWIG++ [42]. A comparison between this sample and a different one produced with Madgraph5_aMC@NLO interfaced to HERWIG++ is used to estimate the uncertainty associated to the matrix-element implementation and the matching to the parton showers. Separate alternative samples are also generated with POWHEG-BOX v2 interfaced to PYTHIA v6.428 with extra jet radiation emitted in the matrix element and in the parton shower. In addition, the modelling of the overlap at NLO between Wt and $t\bar{t}$ diagrams [43] is studied. The effect is assessed by generating Wt events with different schemes for overlap removal using the POWHEG-BOX v2 event generator interfaced to PYTHIA v6.428 for the simulation of parton showering and non-perturbative effects. These samples are simulated following the recommendations documented in Ref. [44]. The $t\bar{t}$ samples are normalised using the NNLO+NNLL soft-gluon resummation prediction [45], while the Wt samples are normalised using the NLO+NNLL prediction [46].

The EvtGen v1.2.0 [47] program is used for the properties of the bottom and charm hadron decays in all samples generated using the POWHEG-BOX v2 and Madgraph5_aMC@NLO v2.2.2 programs. The generated samples are passed through a simulation of the ATLAS detector based on GEANT4 [48,49]. They are overlaid with additional proton–proton interactions (pile-up) generated with PYTHIA v8.210 and the distribution of the average number of interactions per bunch crossing is reweighted to agree with the corresponding data distribution. The simulated events are reconstructed and analysed with the same algorithms as the data and are corrected with data-driven correction factors to account for differences between data and simulation in lepton and jet reconstruction and identification.

4. Event reconstruction and selection

The WW event candidates are selected by requiring exactly one electron and one muon of opposite charge in the event, and significant missing transverse momentum, as described below. Events with a same-flavour lepton pair are not used because they have larger background from the Drell–Yan process.

Candidate events are preselected by either a single-muon or single-electron trigger requiring transverse momentum $p_T > 20$ or 24 GeV respectively. The efficiency of the trigger for selecting WW events is approximately 99% for events that pass the offline selection.

Leptons are required to originate from the primary vertex, defined as the reconstructed vertex with the largest sum of the p_T^2 of the associated tracks. The longitudinal impact parameter of each lepton track, defined as the distance along the beam line between the track and the point of closest approach of the track to the primary vertex, multiplied by the sine of the track θ angle, is required to be less than 0.5 mm. Furthermore, the significance of the transverse impact parameter calculated with respect to the beam line, $|d_0/\sigma_{d_0}|$, is required to be less than 3.0 (5.0) for muons (electrons).

Electron candidates are reconstructed from the combination of a cluster of energy deposits in the electromagnetic calorimeter and a track in the ID [50]. Candidate electrons must satisfy the *Tight* quality definition described in Ref. [50]. Muon candidates are re-

Table 1

Lepton, jet, and event selection criteria for WW candidate events. In the table ℓ stands for e or μ . The definitions of identification and isolation are given in Refs. [50] and [51].

Selection requirement	Selection value
p_T^ℓ	> 25 GeV
η^ℓ	$ \eta^e < 2.47$ (excluding $1.37 < \eta^e < 1.52$), $ \eta^\mu < 2.4$
Lepton identification	Tight (electron), Medium (muon)
Lepton isolation	Gradient working point
Number of additional leptons ($p_T > 10$ GeV)	0
$m_{e\mu}$	> 10 GeV
Number of jets with $p_T > 25(30)$ GeV, $ \eta < 2.5(4.5)$	0
Number of b -tagged jets ($p_T > 20$ GeV, 85% op. point)	0
$E_{T, \text{Rel}}^{\text{miss}}$	> 15 GeV
p_T^{miss}	> 20 GeV

constructed by combining a track in the ID with a track in the MS [51]. The *Medium* criterion, as defined in Ref. [51], is applied to the combined tracks. The leptons are required to be isolated using information from ID tracks and calorimeter energy clusters in a cone around the lepton. The expected isolation efficiency for prompt leptons is at least 90% (99%) at a p_T of 25 (60) GeV using a so-called *gradient* working point [50,51].

Jet candidates are reconstructed within the calorimeter acceptance using the anti- k_t jet clustering algorithm [52] with a radius parameter of $R = 0.4$ which combines clusters of topologically-connected calorimeter cells [53]. The jet energy is calibrated by applying a p_T - and η -dependent correction derived from MC simulation with additional corrections based on data [54]. As part of the jet energy calibration a pile-up correction based on the concept of jet area is applied to the jet candidates [55]. The jet-vertex-tagger (JVT) technique [56] is used to separate hard-scatter jets from pile-up jets within the acceptance of the tracking detector by requiring a significant fraction of the jet's summed track p_T to come from tracks associated with the primary vertex. A jet-vertex-tagger requirement of $\text{JVT} > 0.64$ for jets with $p_T < 50$ GeV and $|\eta| < 2.4$ is applied. This requirement has an efficiency that increases with the jet p_T and is between 87% and 98% for selecting hard-scatter jets with p_T in the range 20–50 GeV. Candidate jets are discarded if they lie within a cone of size $\Delta R = 0.2$ around an electron or, for jets with less than three associated tracks, around a muon candidate. If a jet with three or more associated tracks lies within $\Delta R < 0.4$ of a muon, or $0.2 < \Delta R < 0.4$ of an electron, the corresponding lepton candidate is discarded. Within the ID acceptance, jets originating from the fragmentation of b -hadrons (b -jets) are identified using a multivariate algorithm [57,58]. The chosen operating point has an efficiency of 85% for selecting jets containing b -hadrons and a rejection factor of 28 for light-quark jets, as estimated in a sample of simulated $t\bar{t}$ events and validated with data.

The missing transverse momentum is computed as the negative of the vectorial sum of the transverse momenta of the reconstructed objects selected in the analysis (i.e. electrons, muons, and jets), and a soft term based on the tracks associated with the primary vertex but not with the hard objects explicitly used in the missing transverse momentum computation [59]. The magnitude of the missing transverse momentum is denoted by E_T^{miss} in the following. The jet selection in the E_T^{miss} computation is chosen to provide a compromise between good resolution and scale, with the requirement of $p_T > 20$ GeV for all jets, and an additional $\text{JVT} > 0.64$ requirement for jets in the region of $|\eta| < 2.4$. In Drell–Yan production of τ -lepton pairs with subsequent decay to an $e\mu$ pair, the direction of the missing transverse momentum tends to align with a final-state lepton. To suppress this contamination a requirement is imposed on the missing transverse momentum component perpendicular to the direction in the r - ϕ plane of the lepton closest to the missing transverse momentum

direction, as defined in Ref. [6]. This variable is denoted in the following by $E_{T, \text{Rel}}^{\text{miss}}$. In addition, a more pile-up-robust track-based missing transverse momentum variable of magnitude p_T^{miss} is computed within the ID acceptance [59], using only ID tracks associated with the primary vertex.

The signal region (SR) in which the measurement is performed is defined as follows. Candidate WW events are required to have one electron and one muon, each with $p_T > 25$ GeV, of opposite charge. The electron is required to be in the region $|\eta| < 2.47$, excluding the transition region between the barrel and endcap calorimeters. For the muon, $|\eta| < 2.4$ is required. To reduce the background from other diboson processes, the events are required to have no additional electron or muon with $p_T > 10$ GeV. To suppress the background contribution from top quarks, events are required to have no jets with $p_T > 25$ (30) GeV in $|\eta| < 2.5$ (4.5), and no b -jets with $p_T > 20$ GeV. In addition, the requirements $E_{T, \text{Rel}}^{\text{miss}} > 15$ GeV, $p_T^{\text{miss}} > 20$ GeV, and the invariant mass of the lepton pair $m_{e\mu} > 10$ GeV suppress Drell–Yan background contributions. The lepton, jet, and event selection criteria are summarised in Table 1.

5. Background estimation

After applying the event selection requirements described in Section 4, the dominant background in the WW candidate sample is top-quark ($t\bar{t}$ and single top) production with neither jet nor b -jet above the veto thresholds within the acceptance. Drell–Yan production of a τ -lepton pair that decays leptonically can also give rise to the $e\mu$ final state. Multi-jet production with two jets misidentified as leptons, or W + jets production with leptonic W decay and a jet misidentified as a lepton (collectively referred to as W + jets background below) can be mistakenly accepted as candidate events. This background category includes events where an electron or a muon is produced from a semileptonic decay of a bottom or charm hadron and WW events where one W decays leptonically and the other hadronically. Other diboson (WZ , ZZ , $W\gamma$ and $Z\gamma$) production contributes a smaller background. Minor background processes are modelled with MC simulations, while data-driven methods are used to determine the dominant backgrounds and backgrounds with a misidentified lepton. The normalisations of top-quark and Drell–Yan backgrounds are determined from dedicated control regions after a simultaneous fit, described in detail in Section 8. The phase spaces of top-quark and Drell–Yan control regions are chosen to be close to the one of the signal region. Modelling uncertainties for each of the backgrounds, discussed here, as well as the systematic and statistical uncertainties given in Section 8, are included as nuisance parameters in the fit.

The top-quark background control region is defined by requiring one jet with $p_T > 25$ GeV and at least one b -jet with

$p_T > 20$ GeV in the ID acceptance region of $|\eta| < 2.5$, in an event sample selected with the same lepton criteria as the signal region and no requirement on $E_{T, \text{Rel}}^{\text{miss}}$. This control region has an estimated top purity of 93%. The top-quark background, comprising $t\bar{t}$ and Wt contributions, is normalised to data in this control region and both the detector and modelling uncertainties affect the extrapolation of $t\bar{t}$ and Wt from the control region to the signal region. These include $t\bar{t}$ (Wt) cross section uncertainties of 6% (10%) as well as the modelling of the parton shower and initial-state jet radiation. For the $t\bar{t}$ process the uncertainties also include the choice of MC matrix-element generator, while for the Wt process they include the modelling of the overlap and interference at NLO between Wt and $t\bar{t}$ diagrams estimated by comparing the nominal Wt MC sample with an alternative sample generated with a different scheme for overlap removal. The uncertainties in modelling the $t\bar{t}$ and Wt processes are estimated by comparing the results from the different MC samples presented in Section 3.

The event characteristics of $e\mu$ final states from Drell–Yan production of τ -lepton pairs include an $e\mu$ invariant mass below the Z mass, and lower $E_{T, \text{Rel}}^{\text{miss}}$. In the Drell–Yan background control region, the $e\mu$ invariant mass is required to be $45 < m_{e\mu} < 80$ GeV, and either or both of the $E_{T, \text{Rel}}^{\text{miss}}$ and p_T^{miss} requirements are reversed to make the sample orthogonal to that in the signal region while all other selection requirements remain the same. The Drell–Yan control region has a purity of about 95%, and the Drell–Yan modelling uncertainties are taken into account by comparing different MC event generators, as discussed in Section 3.

Determining the background from W + jets production requires good knowledge of the lepton misidentification rate, which is best derived from data. The yield from W + jets production is estimated using data event samples that are selected with different lepton selection criteria: a loose lepton identification criterion is defined, leptons are selected using either the loose or the default (as used in the signal region) lepton identification criteria, and events are classified according to whether the leptons, that all satisfy the loose criteria, satisfy or not the default identification criteria. With the introduction of the efficiencies of the default lepton identification relative to the loose lepton identification for both real and misidentified leptons, a system of four equations can be solved to estimate the number of events meeting the default lepton identification criteria. This follows the same procedure as that described in Ref. [6]. For electrons, the loose identification corresponds to the *medium* criterion defined in Ref. [50] without isolation requirements. For muons, the loose identification is the same as the default one, except that the isolation requirement is omitted. The efficiencies for jet misidentification are determined for electrons and muons separately as a function of the lepton p_T and are cross-checked with a two-dimensional parameterisation in the lepton p_T and η . These efficiencies are measured using data in a control region with one lepton, at least one jet and requirements on the lepton- $E_{T, \text{Rel}}^{\text{miss}}$ transverse mass and E_T^{miss} to suppress the prompt-lepton contribution from W + jet production. The remaining W + jets contribution in the selected control sample is subtracted using the MC prediction. The efficiencies for real leptons are determined from WW MC simulations with correction factors obtained by comparing $Z \rightarrow \ell\ell$ events in data and MC simulation. The systematic uncertainties for lepton misidentification include variations of the control region definition, the cross section uncertainties used for the subtraction of the contributions from real leptons, and the method bias (non-closure), which is estimated by comparing the prediction for the W + jet background contribution from MC simulation with the result of the experimental method applied to the same MC sample.

The estimate of the diboson background from WZ , ZZ , $W\gamma$ and $Z\gamma$ processes is based on MC simulation. The diboson back-

Table 2Definition of the $WW \rightarrow e\mu$ fiducial phase space, where $\ell = e$ or μ .

Fiducial selection requirement	Cut value
p_T^ℓ	> 25 GeV
$ \eta_\ell $	< 2.5
$m_{e\mu}$	> 10 GeV
Number of jets with $p_T > 25(30)$ GeV, $ \eta < 2.5(4.5)$	0
$E_{T, \text{Rel}}^{\text{miss}}$	> 15 GeV
E_T^{miss}	> 20 GeV

ground uncertainty is estimated by comparing the yields of the dominant process, WZ , predicted by two different event generators, SHERPA and POWHEG-BOX, for which a difference of 30% is observed. Such uncertainty is then applied to the whole diboson contribution.

The observed numbers of events in the signal region, and the top-quark and Drell–Yan control regions, are shown later in Table 3.

6. Fiducial cross-section definition

The WW cross section is evaluated in the fiducial phase space of the $e\mu$ decay channel. The fiducial phase space is defined in Table 2 as selection criteria for MC events with no detector simulation. Electrons and muons are required at particle level to stem from one of the W bosons produced in the hard scatter and their respective momenta after QED final-state radiation are vectorially added to the momenta of photons emitted in a cone of size $\Delta R = 0.1$ around the lepton direction. Final-state particles with lifetime greater than 30 ps are clustered into jets (referred to as particle-level jets) using the same algorithm as for detector-level jets, i.e. with the anti- k_t algorithm with radius parameter $R = 0.4$. The selected charged leptons and neutrinos from W -boson decays are not included in the jet clustering. The fiducial phase space at particle level does not make any requirement on b -quark jets. The missing transverse momentum is defined at particle level as the transverse component of the vectorial sum of the neutrino momenta. In Table 2, the missing transverse momentum magnitude is denoted as E_T^{miss} , while its component perpendicular to the closest lepton in the r - ϕ plane is denoted as $E_{T, \text{Rel}}^{\text{miss}}$.

The fiducial cross section is defined as

$$\sigma_{WW \rightarrow e\mu}^{\text{fid}} = \frac{N_{\text{obs}} - N_{\text{bkg}}}{C \times \mathcal{L}}, \quad (1)$$

where \mathcal{L} is the integrated luminosity, N_{obs} is the observed number of events, N_{bkg} is the estimated number of background events and C is a factor that accounts for detector inefficiencies and contributions from τ -lepton decays. The factor C is estimated in simulation as the ratio of the number of signal events with one electron and one muon (including those from τ decays) passing the selection requirements at detector level listed in Section 4 to those passing the fiducial selection (excluding $W \rightarrow \tau\nu$ decays) at particle level. Therefore C implicitly corrects for the contribution of $W \rightarrow \tau\nu$ decays, which is estimated in MC simulations to be 8%, based on their acceptance relative to the signal $WW \rightarrow e\mu$ channel and the relative branching fractions from the MC simulation.

7. Systematic uncertainties

Systematic uncertainties in the WW cross-section measurement in the fiducial phase space arise from the reconstruction of leptons and jets, the background determination, pile-up and luminosity uncertainties, and the procedures used to correct for detector effects.

The uncertainty in the C factor in Eq. (1) is dominated by experimental sources. Uncertainties in the lepton and jet reconstruction affect the signal acceptance in the fiducial phase space. The effects are estimated by varying the energy or momentum scale and the resolution of leptons and jets, and the correction factors for the trigger, reconstruction, identification and isolation efficiencies, within their uncertainties estimated in dedicated data analyses [50, 51, 54]. Uncertainties in the E_T^{miss} reconstruction and b -tagging are also taken into account based on the studies in Ref. [59] and Ref. [57] respectively. The impact of the hard-object uncertainties in the E_T^{miss} is estimated by individually varying each of their associated uncertainties and recalculating E_T^{miss} for each variation. In addition, uncertainties in the scale and resolution of the E_T^{miss} soft term are estimated using data as discussed in Refs. [59] and [60].

The full set of detector-related uncertainties is taken into account in the background estimation. The statistical uncertainties stemming from the size of the MC samples used for the background estimates and from the size of the data samples used for data-driven estimations in the control regions are also considered as systematic uncertainties. The uncertainties due to the modelling of background processes in the signal and control regions are estimated by comparing different event generators, as discussed in Sections 3 and 5.

The MC samples are reweighted to reproduce the distributions in data of the average number of interactions per bunch crossing, and additionally the number of reconstructed primary vertices per event. The uncertainty due to pile-up is estimated as the difference between the two. An uncertainty of 2.1% in the integrated luminosity affects the cross-section measurement and the MC-based estimate of backgrounds. It is determined following the same methodology as that detailed in Ref. [61] based on a calibration of the luminosity scale using x - y beam-separation scans performed in August 2015. The beam energy uncertainty of 0.66% (from Ref. [62]) gives a 1.7% uncertainty in the theoretical cross section, which is not accounted for in the predictions quoted in this Letter.

Uncertainties in the C factor due to theoretical sources are also included. The uncertainties associated with PDFs are taken as the largest of either the CT10 NLO eigenvector uncertainty band at 68% confidence level, or the difference among the central values of CT10 NLO, MSTW2008nlo [63] and NNPDF3.0 [64] PDFs. The uncertainty associated with higher-order QCD corrections is estimated by varying renormalisation (μ_R) and factorisation (μ_F) scales independently by factors of 2 and 0.5 with the constraint $0.5 \leq \mu_F/\mu_R \leq 2$. The effects of parton shower, hadronisation and underlying event models (referred to here as *parton shower* for simplicity) are accounted for by comparing the default MC prediction for WW production, which uses PYTHIA v8.210 for modelling of these effects, with the prediction obtained with the models implemented in HERWIG++.

A full list of systematic uncertainties and their impact on the cross-section measurement is given in Table 4.

8. The fiducial cross-section measurement

The fiducial cross section $\sigma_{WW \rightarrow e\mu}^{\text{fid}}$ is extracted by minimising a negative log-likelihood function, based on observed and expected numbers of events in the signal region, as defined by the signal event selection, and in the top-quark and Drell-Yan control regions, as defined in Section 5. The likelihood consists of a product of Poisson probability density functions for the orthogonal regions. This procedure allows a simultaneous measurement of the signal process cross section and of the contributions from the top-quark and Drell-Yan processes. Systematic uncertainties are taken into account as constrained nuisance parameters in the log-likelihood

Table 3

Observed number of events in data and estimated numbers of events from signal and background processes in the signal and control regions. The numbers of events from signal and background processes are the result of the simultaneous fit, i.e. are constrained to match the data in the signal and control regions. The quoted uncertainties account for statistical and systematic components on the number of events for each process and do not include the uncertainties in the C factor. The correlations among processes for common systematic uncertainties are accounted for in the total uncertainties.

Process	Signal region	Top-quark control region	Drell-Yan control region
WW signal	997 ± 69	49 ± 12	75.3 ± 5.4
Drell-Yan	62 ± 23	49 ± 29	1568 ± 45
$t\bar{t}$ + single top	177 ± 33	2057 ± 81	3.5 ± 1.6
W + jets/multi-jet	78 ± 41	70 ± 55	0 ± 17
Other dibosons	38 ± 12	6.3 ± 3.5	19.2 ± 6.1
Total	1351 ± 37	2232 ± 47	1666 ± 41
Data	1351	2232	1666

Table 4

Breakdown of the relative uncertainties in the fiducial cross-section measurement as a result of the simultaneous fit to signal and control regions. “Electron” and “Muon” uncertainties include contributions from trigger, energy/momentum reconstruction, identification and isolation.

Sources of uncertainty	Relative uncertainty for $\sigma_{WW \rightarrow e\mu}^{\text{fid}}$
Jet selection and energy scale & resolution	7.3%
b -tagging	1.3%
E_T^{miss} and p_T^{miss}	1.7%
Electron	1.0%
Muon	0.4%
Pile-up	0.9%
Luminosity	2.1%
Top-quark background theory	2.4%
Drell-Yan background theory	1.5%
W + jet and multi-jet background	3.8%
Other diboson backgrounds	1.1%
Parton shower	3.1%
PDF	0.2%
QCD scale	0.2%
MC statistics	1.2%
Data statistics	3.7%
Total uncertainty	11%

function. The methodology accounts for uncertainties and their correlations across signal and background processes. It is found that the Drell-Yan and top-quark processes need to be scaled relative to their MC predictions by 1.03 ± 0.03 and 0.875 ± 0.035 respectively to match the observed data yields in the corresponding control regions. The uncertainties of the quoted scale factors are driven by the data statistics in the respective control regions and do not include modelling uncertainties on the respective processes. The number of events observed in data and the estimated numbers of signal and background events together with their total uncertainties are reported in Table 3. The correction factor C is calculated to be 0.60 ± 0.04 , where the uncertainty accounts for the systematic effects discussed in Section 7. The measured signal cross section is

$$\sigma_{WW \rightarrow e\mu}^{\text{fid}} = 529 \pm 20 \text{ (stat.)} \pm 50 \text{ (syst.)} \pm 11 \text{ (lumi.) fb.}$$

The total uncertainty is dominated by systematic sources, as described in Section 7, of which the largest contribution originates from the experimental jet selection and calibration. The correlations of the fit parameters in the signal and control regions are taken into account in the computation of the total uncertainties.

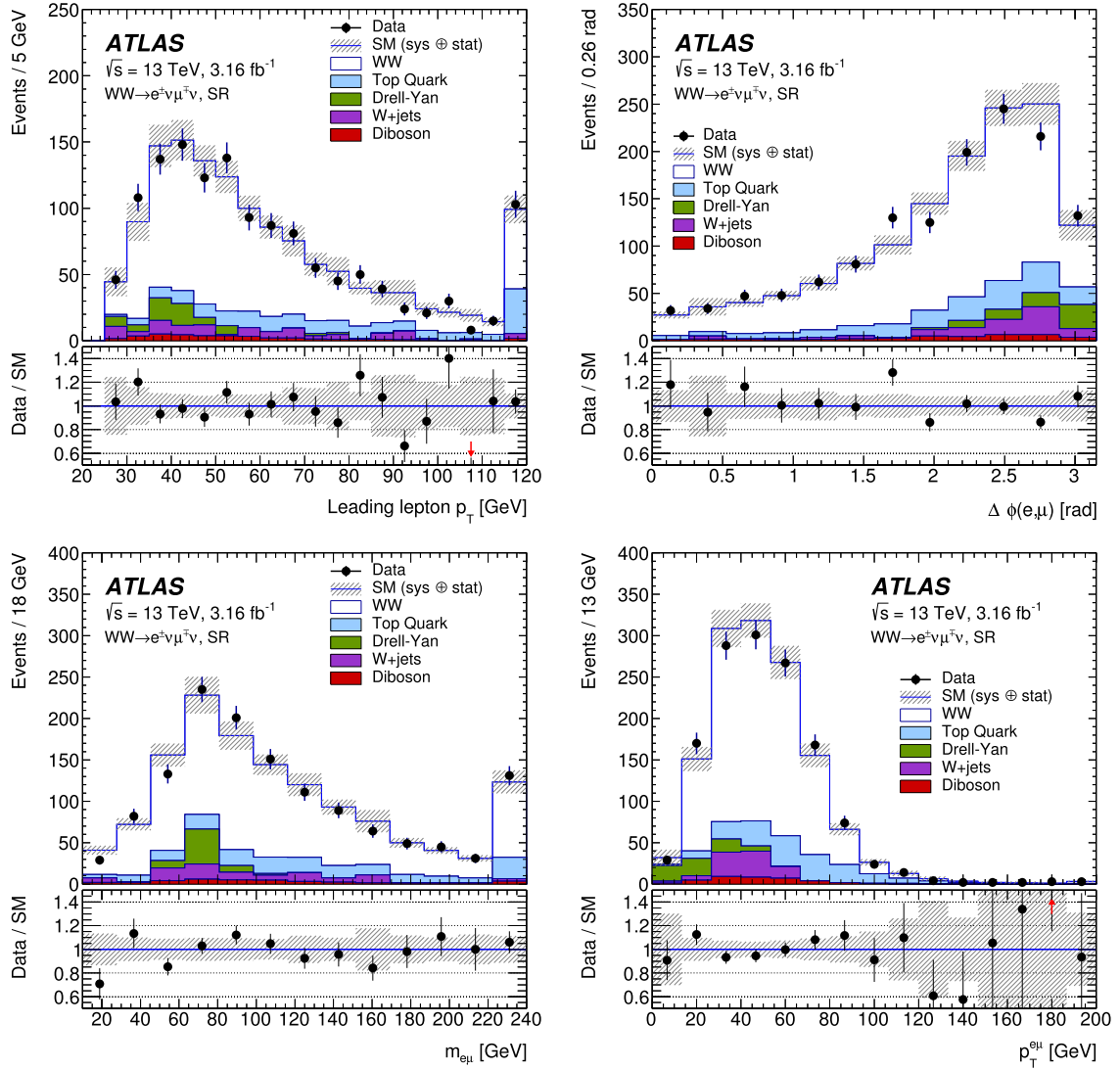


Fig. 1. Lepton and dilepton kinematic variables in the signal region. In the figure $m_{e\mu}$ and $p_T^{e\mu}$ are the invariant mass and the transverse momentum of the $e\mu$ system respectively, and $\Delta\phi(e, \mu)$ is the azimuthal angle between the two leptons. Data are shown together with the MC and data-driven predictions for the signal and background production processes after the fit to the data in the signal and control regions. The last bin in each distribution is the overflow. In the legend, SM stands for the total contribution of the estimated SM processes and the uncertainty band includes the MC statistical and systematic uncertainties as a result of the fit.

The contributions to the relative uncertainty in the fiducial cross-section measurement are summarised in Table 4. Fig. 1 shows distributions of kinematic variables from data events in the signal region in comparison with the signal and background contributions estimated from the simultaneous fit to signal and control regions.

9. Theoretical predictions and ratio to the 8 TeV measurement

Theoretical predictions are calculated in the total phase space (σ_{WW}^{tot}) and include the $q\bar{q} \rightarrow WW$, the non-resonant $gg \rightarrow WW$, and the resonant $gg \rightarrow H \rightarrow WW$ sub-processes. The $q\bar{q} \rightarrow WW$ production cross section is known to $\mathcal{O}(\alpha_s^2)$ (NNLO) [9, 13], the non-resonant gg sub-process is known to $\mathcal{O}(\alpha_s^3)$ [33], and the resonant $gg \rightarrow H \rightarrow WW$ cross section is calculated to $\mathcal{O}(\alpha_s^5)$ [65] taking into account the $H \rightarrow WW$ branching fraction [66]. The sum of these sub-processes is denoted by nNNLO+H in the following. In its calculation, the interference between the three sub-processes is neglected. At the given orders of α_s listed above, the $q\bar{q} \rightarrow WW$ process does not interfere with either of the gg -induced processes and the interference between the

gg -induced processes has little contribution to the cross section in the measured phase space. As in the 8 TeV cross-section measurement, possible contributions from double parton interactions are not considered as their contribution is expected to be negligible [6].

The renormalisation and factorisation scales are set to the W boson mass for the $q\bar{q}$ and non-resonant gg processes, and to $m_H/2$ for $gg \rightarrow H \rightarrow WW$. The uncertainties in the $q\bar{q} \rightarrow WW$ cross section are estimated by varying the two scales independently by factors of 0.5 and 2 with the constraint $0.5 \leq \mu_F/\mu_R \leq 2$, while the uncertainties in the non-resonant and resonant gg cross sections are estimated by simultaneously varying μ_R and μ_F by factors of 0.5 and 2. The uncertainties in $gg \rightarrow WW$ and $gg \rightarrow H \rightarrow WW$ processes include a 3.2% contribution from PDF uncertainties computed in Ref. [67]. For the $q\bar{q} \rightarrow WW$ process, PDF uncertainties are estimated as the largest of either the CT10 NLO eigenvector uncertainty band (at 68% confidence level) or the difference among the central values of CT10 NLO, MSTW2008nlo and NNPDF3.0 PDFs, amounting to 1.8%. The uncertainties associated with the individual sub-processes are propa-

Table 5

Theoretical predictions for the WW cross-section sub-processes and their associated uncertainties in the full phase space (σ_{WW}^{tot}) calculated up to the given order in α_s together with the respective acceptance corrections (A) for the fiducial phase space and the fiducial cross sections ($\sigma_{WW \rightarrow e\mu}^{\text{fid}}$). The resonant $gg \rightarrow H \rightarrow WW$ is calculated up to $\mathcal{O}(\alpha_s^5)$ for σ_{WW}^{tot} and to $\mathcal{O}(\alpha_s^3)$ for $\sigma_{WW \rightarrow e\mu}^{\text{fid}}$ and A . A correction is applied to $\sigma_{WW \rightarrow e\mu}^{\text{fid}}$ and A to account for non-perturbative effects. The quoted uncertainties include scale variations and PDF uncertainties, with the latter being evaluated at NLO. The scale uncertainties are treated as correlated, whereas PDF uncertainties are treated as uncorrelated between the $q\bar{q}$ and the gg -induced processes. The values of the branching ratio of leptonic W -boson decay used for each sub-process are those reported in their respective References, while for the resonant gg sub-process $\mathcal{B} = 0.1083$ [69] is used.

$pp \rightarrow WW$ sub-process	Order of α_s	σ_{WW}^{tot} [pb]	A [%]	$\sigma_{WW \rightarrow e\mu}^{\text{fid}}$ [fb]
$q\bar{q}$ [9,13]	$\mathcal{O}(\alpha_s^2)$	111.1 ± 2.8	16.20 ± 0.13	422^{+12}_{-11}
gg (non-resonant) [33]	$\mathcal{O}(\alpha_s^3)$	$6.82^{+0.42}_{-0.55}$	$28.1^{+2.7}_{-2.3}$	44.9 ± 7.2
$gg \rightarrow H \rightarrow WW$ [68][30]	$\mathcal{O}(\alpha_s^5)$ tot. / $\mathcal{O}(\alpha_s^3)$ fid.	$10.45^{+0.61}_{-0.79}$	4.5 ± 0.6	11.0 ± 2.1
$q\bar{q} + gg$ (non-resonant) + $gg \rightarrow H \rightarrow WW$	nNNLO+H	$128.4^{+3.5}_{-3.8}$	$15.87^{+0.17}_{-0.14}$	478 ± 17

gated to the σ_{WW}^{tot} prediction for the nNNLO+H combination: scale uncertainties of different processes are added linearly, while PDF uncertainties are considered uncorrelated across processes. The $q\bar{q}$ production makes up 87% of the total cross section while the non-resonant and resonant gg production sub-processes account for 5% and 8% respectively.

For direct comparison to the experimental result, theoretical predictions are also calculated in the same phase space as the measurement ($\sigma_{WW \rightarrow e\mu}^{\text{fid}}$) for the $q\bar{q}$ and non-resonant gg processes. A correction of 0.972 ± 0.001 is applied to parton-level calculations for $\sigma_{WW \rightarrow e\mu}^{\text{fid}}$ to account for the contribution of non-perturbative effects due to multi-parton interactions and hadronisation. This correction was calculated by comparing the particle-level cross section as predicted by the MC simulation with one obtained with a dedicated event generation where these effects are disabled in PYTHIA v8.210. The uncertainty includes the MC statistical uncertainty and the systematic component estimated by comparing the above correction with the one estimated with the non-perturbative model implemented in the HERWIG++ MC event generator. The calculations reported here do not include high-order electroweak corrections. In Ref. [70] it is estimated that electroweak corrections up to NLO reduce the WW cross section by 3–4% in a phase space close to the one used in this analysis. The $q\bar{q}$ and non-resonant gg fiducial cross sections are calculated with the programs presented in Refs. [9,13] and [33] respectively. For the resonant $gg \rightarrow H \rightarrow WW$ process, no fiducial calculation is available at $\mathcal{O}(\alpha_s^5)$. Therefore, this fiducial cross section is calculated by correcting the cross section in the full phase space (σ_{WW}^{tot}) by the geometrical and kinematic acceptance A as determined using the MC event generator POWHEG-BOX v2 interfaced to PYTHIA v8.210 for parton showering and non-perturbative effects and the branching ratio (\mathcal{B}) for fully leptonic final states, $\mathcal{B} = 0.1083$ [69]:

$$\sigma_{WW \rightarrow e\mu}^{\text{fid}} = 2 \times \sigma_{WW}^{\text{tot}} \times A \times \mathcal{B}^2. \quad (2)$$

In this determination of the $gg \rightarrow H \rightarrow WW$ fiducial cross section, uncertainties from PDFs and scale uncertainties are considered for both A and σ_{WW}^{tot} , while parton shower uncertainties are also estimated for A . The $q\bar{q}$ and non-resonant gg acceptances are calculated using the ratios of the respective fiducial cross section to the total cross section. The uncertainties in the A factors for $q\bar{q}$ and non-resonant gg processes are estimated following the same methodology as for σ_{WW}^{tot} and considering both the scale and PDF uncertainties as correlated between $\sigma_{WW \rightarrow e\mu}^{\text{fid}}$ and σ_{WW}^{tot} . The total uncertainty in A in the nNNLO+H calculation is then determined from the propagation of the A factor uncertainties for the individual sub-processes. The PDF uncertainties are found to be dominant and to lead to an uncertainty of 2.5% and 3.2% on A for the $q\bar{q}$ and gg sub-processes respectively.

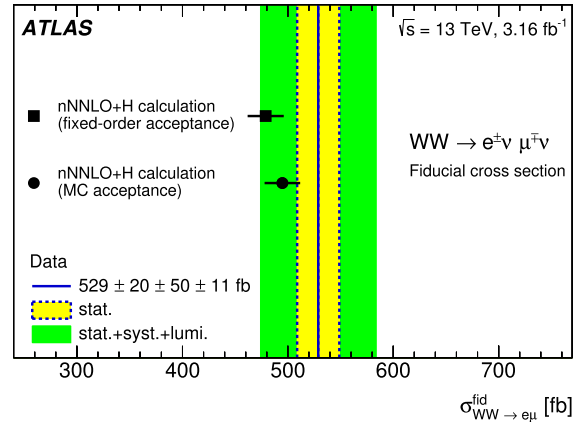


Fig. 2. The measured fiducial cross section at $\sqrt{s}=13$ TeV in comparison with the nNNLO+H prediction in the fiducial phase space with two different acceptance calculations. The vertical bands around the measurement indicate the statistical uncertainty (yellow) and the sum in quadrature of statistical, systematic and luminosity uncertainties (green). The beam energy uncertainty is not taken into account.

The theoretical cross-section predictions for each production sub-process and the nNNLO+H combination in the total and fiducial phase spaces as well as the A factors (corrected for non-perturbative effects) are given together with their estimated uncertainties in Table 5. Fig. 2 shows the comparison of the nNNLO+H prediction with the measurement presented in the previous section. Fig. 2 also reports, as an alternative prediction, the σ_{WW}^{tot} calculation for the nNNLO+H combination corrected by the acceptance A calculated using the MC event generator POWHEG-BOX v2 + PYTHIA v8.210 for the $q\bar{q}$ and resonant $gg \rightarrow H \rightarrow WW$ processes, and SHERPA v2.1.1 for the non-resonant gg process. In this calculation the acceptance factor is estimated to be $A = (16.4 \pm 0.9)\%$ where the uncertainty includes the parton shower modelling (taken as the difference between PYTHIA v8.210 and HERWIG++ showers), PDF uncertainty (estimated as the largest difference between the CT10 NLO eigenvector uncertainty band and the MSTW2008nlo and NNPDF3.0PDF central values), scale uncertainty associated with the jet veto requirement estimated as in Ref. [71] and the residual renormalisation and factorisation scale uncertainty (estimated by varying the two scales independently by factors of 2 and 0.5).

The nNNLO+H prediction agrees within uncertainties with the experimental cross-section measurement in the fiducial phase space.

The cross section in the full phase space (σ_{WW}^{tot}) is determined by extrapolating the measurement in the fiducial phase space by inverting Eq. (2) and using the acceptance value from the nNNLO+H calculation as in Table 5: $\sigma_{WW}^{\text{tot}} = 142 \pm 5$ (stat.) \pm

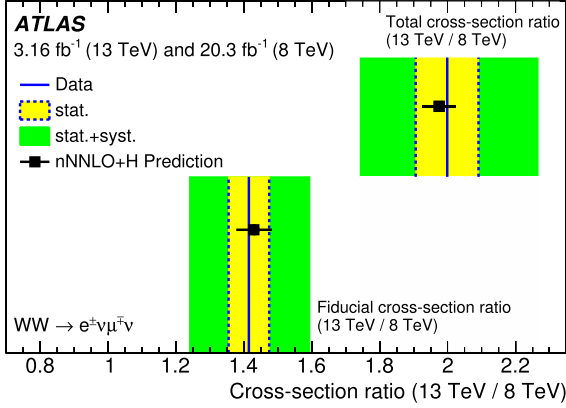


Fig. 3. Measurements of the ratios of cross sections at the two centre-of-mass energies of 13 and 8 TeV in the fiducial and total phase spaces. For the 8 TeV cross sections the results from Ref. [6] are used. The measurements are compared to the nNNLO+H predictions for the ratios of cross sections in the fiducial phase spaces of the two analyses at 13 and 8 TeV and in the total phase space, with their respective uncertainties. The beam energy uncertainty is not taken into account.

$13 \text{ (syst.)} \pm 3 \text{ (lumi.) pb}$. This is in agreement with the nNNLO+H prediction of $128.4^{+3.5}_{-3.8} \text{ pb}$.

Using the fiducial cross section measured for $WW \rightarrow e\mu$ production at 8 TeV centre-of-mass energy [6] in the fiducial phase space detailed in Ref. [6], the ratio of cross sections at the two centre-of-mass energies of 13 and 8 TeV is:

$$\frac{\sigma_{13 \text{ TeV}, WW \rightarrow e\mu}^{\text{fid}}}{\sigma_{8 \text{ TeV}, WW \rightarrow e\mu}^{\text{fid}}} = 1.41 \pm 0.06 \text{ (stat.)} \pm 0.16 \text{ (syst.)} \pm 0.04 \text{ (lumi.)}.$$

All uncertainties are treated as uncorrelated between the measurements at the two beam energies: no attempt is made to exploit the jet energy scale correlations between the two data-taking periods at different beam energies. The same ratio is calculated for the total cross sections at 13 and 8 TeV and is found to be $2.00 \pm 0.08 \text{ (stat.)}^{+0.25}_{-0.24} \text{ (syst.)} \pm 0.06 \text{ (lumi.)}$. Fig. 3 shows the measured ratios of cross sections in the fiducial and total phase spaces and the comparison with their respective nNNLO+H predictions with scale uncertainties treated as correlated between the two centre-of-mass energies, while the PDF uncertainties are considered uncorrelated. The predictions for the ratio in the fiducial and total phase spaces are 1.43 ± 0.05 and 1.98 ± 0.05 respectively, and are in agreement with the experimental results.

10. Conclusions

The cross section for production of W^+W^- pairs in pp collisions at $\sqrt{s} = 13 \text{ TeV}$ is measured in a fiducial phase space of the $e\mu$ final state in which events with reconstructed jets are excluded. The data used in the analysis correspond to an integrated luminosity of 3.16 fb^{-1} collected by the ATLAS detector at the LHC in 2015. The measurement is made in a relatively pure signal region with the contamination from the dominant background processes estimated using data in dedicated control regions. The measured cross section is $529 \pm 20 \text{ (stat.)} \pm 50 \text{ (syst.)} \pm 11 \text{ (lumi.) fb}$ and is found to be consistent with the most up-to-date SM predictions that include high-order QCD effects. Furthermore, the ratio of the measured fiducial cross sections at 13 and 8 TeV centre-of-mass energies is compared to the theory predictions with reduced uncertainties, thanks to their cancellation in the ratio.

Acknowledgements

We thank CERN for the very successful operation of the LHC, as well as the support staff from our institutions without whom ATLAS could not be operated efficiently.

We acknowledge the support of ANPCyT, Argentina; YerPhI, Armenia; ARC, Australia; BMWFW and FWF, Austria; ANAS, Azerbaijan; SSTC, Belarus; CNPq and FAPESP, Brazil; NSERC, NRC and CFI, Canada; CERN; CONICYT, Chile; CAS, MOST and NSFC, China; COLCIENCIAS, Colombia; MSMT CR, MPO CR and VSC CR, Czech Republic; DNRF and DNSRC, Denmark; IN2P3-CNRS, CEA-DSM/IRFU, France; SRNSF, Georgia; BMBF, HGF, and MPG, Germany; GSRT, Greece; RGC, Hong Kong SAR, China; ISF, I-CORE and Benoziyo Center, Israel; INFN, Italy; MEXT and JSPS, Japan; CNRST, Morocco; NWO, Netherlands; RCN, Norway; MNiSW and NCN, Poland; FCT, Portugal; MNE/IFA, Romania; MES of Russia and NRC KI, Russian Federation; JINR; MESTD, Serbia; MSSR, Slovakia; ARRS and MIZŠ, Slovenia; DST/NRF, South Africa; MINECO, Spain; SRC and Wallenberg Foundation, Sweden; SERI, SNSF and Cantons of Bern and Geneva, Switzerland; MOST, Taiwan; TAEK, Turkey; STFC, United Kingdom; DOE and NSF, United States of America. In addition, individual groups and members have received support from BCKDF, the Canada Council, CANARIE, CRC, Compute Canada, FQRNT, and the Ontario Innovation Trust, Canada; EPLANET, ERC, ERDF, FP7, Horizon 2020 and Marie Skłodowska-Curie Actions, European Union; Investissements d'Avenir Labex and Idex, ANR, Région Auvergne and Fondation Partager le Savoir, France; DFG and AvH Foundation, Germany; Herakleitos, Thales and Aristeia programmes co-financed by EU-ESF and the Greek NSRF; BSF, GIF and Minerva, Israel; BRF, Norway; CERCA Programme Generalitat de Catalunya, Generalitat Valenciana, Spain; the Royal Society and Leverhulme Trust, United Kingdom.

The crucial computing support from all WLCG partners is acknowledged gratefully, in particular from CERN, the ATLAS Tier-1 facilities at TRIUMF (Canada), NDGF (Denmark, Norway, Sweden), CC-IN2P3 (France), KIT/GridKA (Germany), INFN-CNAF (Italy), NL-T1 (Netherlands), PIC (Spain), ASGC (Taiwan), RAL (UK) and BNL (USA), the Tier-2 facilities worldwide and large non-WLCG resource providers. Major contributors of computing resources are listed in Ref. [72].

References

- [1] ALEPH, DELPHI, L3 and OPAL Collaborations, the LEP Electroweak Working Group, S. Schael, et al., Electroweak measurements in electron-positron collisions at W-boson-pair energies at LEP, Phys. Rep. 532 (2013) 119, arXiv:1302.3415 [hep-ex].
- [2] CDF Collaboration, F. Abe, et al., Observation of W^+W^- production in $p\bar{p}$ collisions at $\sqrt{s} = 1.8 \text{ TeV}$, Phys. Rev. Lett. 78 (1997) 4536.
- [3] CDF Collaboration, T. Aaltonen, et al., Measurement of the W^+W^- production cross section and search for anomalous $WW\gamma$ and WWZ couplings in $p\bar{p}$ collisions at $\sqrt{s} = 1.96 \text{ TeV}$, Phys. Rev. Lett. 104 (2010) 201801, Erratum: Phys. Rev. Lett. 105 (2010) 019905, arXiv:0912.4500 [hep-ex].
- [4] D0 Collaboration, V.M. Abazov, et al., Measurement of the WW production cross section with dilepton final states in $p\bar{p}$ collisions at $\sqrt{s} = 1.96 \text{ TeV}$ and limits on anomalous trilinear gauge couplings, Phys. Rev. Lett. 103 (2009) 191801, arXiv:0904.0673 [hep-ex].
- [5] ATLAS Collaboration, Measurement of W^+W^- production in pp collisions at $\sqrt{s} = 7 \text{ TeV}$ with the ATLAS detector and limits on anomalous WWZ and $WW\gamma$ couplings, Phys. Rev. D 87 (2013) 112001, Erratum: Phys. Rev. D 88 (2013) 079906, arXiv:1210.2979 [hep-ex].
- [6] ATLAS Collaboration, Measurement of total and differential W^+W^- production cross sections in proton-proton collisions at $\sqrt{s} = 8 \text{ TeV}$ with the ATLAS detector and limits on anomalous triple-gauge-boson couplings, J. High Energy Phys. 09 (2016) 029, arXiv:1603.01702 [hep-ex].
- [7] CMS Collaboration, Measurement of the W^+W^- cross section in pp collisions at $\sqrt{s} = 7 \text{ TeV}$ and limits on anomalous $WW\gamma$ and WWZ couplings, Eur. Phys. J. C 73 (2013) 2610, arXiv:1306.1126 [hep-ex].

- [8] CMS Collaboration, Measurement of the W^+W^- cross section in pp collisions at $\sqrt{s} = 8$ TeV and limits on anomalous gauge couplings, *Eur. Phys. J. C* 76 (2016) 401, arXiv:1507.03268 [hep-ex].
- [9] T. Gehrmann, et al., W^+W^- production at hadron colliders in next to next to leading order QCD, *Phys. Rev. Lett.* 113 (2014) 212001, arXiv:1408.5243 [hep-ph].
- [10] P. Meade, H. Ramani, M. Zeng, Transverse momentum resummation effects in W^+W^- measurements, *Phys. Rev. D* 90 (2014) 114006, arXiv:1407.4481 [hep-ph].
- [11] P. Jaiswal, T. Okui, An explanation of the WW excess at the LHC by jet-veto resummation, *Phys. Rev. D* 90 (2014) 073009, arXiv:1407.4537 [hep-ph].
- [12] P.F. Monni, G. Zanderighi, On the excess in the inclusive $W^+W^- \rightarrow l^+l^- \nu\bar{\nu}$ cross section, *J. High Energy Phys.* 05 (2015) 013, arXiv:1410.4745 [hep-ph].
- [13] M. Grazzini, S. Kallweit, S. Pozzorini, D. Rathlev, M. Wiesemann, W^+W^- production at the LHC: fiducial cross sections and distributions in NNLO QCD, *J. High Energy Phys.* 08 (2016) 140, arXiv:1605.02716 [hep-ph].
- [14] S. Dawson, P. Jaiswal, Y. Li, H. Ramani, M. Zeng, Resummation of jet veto logarithms at $N^3LL_a + NNLO$ for W^+W^- production at the LHC, *Phys. Rev. D* 94 (2016) 114014, arXiv:1606.01034 [hep-ph].
- [15] ATLAS Collaboration, The ATLAS experiment at the CERN large hadron collider, *J. Instrum.* 3 (2008) S08003.
- [16] ATLAS Collaboration, ATLAS Insertable B-Layer Technical Design Report, ATLAS-TDR-19, url: <https://cds.cern.ch/record/1291633>, 2010, ATLAS Insertable B-Layer Technical Design Report Addendum, ATLAS-TDR-19-ADD-1, url: <https://cds.cern.ch/record/1451888>, 2012.
- [17] P. Nason, A new method for combining NLO QCD with shower Monte Carlo algorithms, *J. High Energy Phys.* 11 (2004) 040, arXiv:hep-ph/0409146.
- [18] S. Frixione, P. Nason, C. Oleari, Matching NLO QCD computations with parton shower simulations: the POWHEG method, *J. High Energy Phys.* 11 (2007) 070, arXiv:0709.2092 [hep-ph].
- [19] S. Alioli, P. Nason, C. Oleari, E. Re, A general framework for implementing NLO calculations in shower Monte Carlo programs: the POWHEG BOX, *J. High Energy Phys.* 06 (2010) 043, arXiv:1002.2581 [hep-ph].
- [20] T. Melia, P. Nason, R. Rontsch, G. Zanderighi, W^+W^- , WZ and ZZ production in the POWHEG BOX, *J. High Energy Phys.* 11 (2011) 078, arXiv:1107.5051 [hep-ph].
- [21] P. Nason, G. Zanderighi, W^+W^- , WZ and ZZ production in the POWHEG-BOX-V2, *Eur. Phys. J. C* 74 (2014) 2702, arXiv:1311.1365 [hep-ph].
- [22] H.-L. Lai, et al., New parton distributions for collider physics, *Phys. Rev. D* 82 (2010) 074024, arXiv:1007.2241 [hep-ph].
- [23] T. Sjöstrand, et al., An introduction to PYTHIA 8.2, *Comput. Phys. Commun.* 191 (2015) 159, arXiv:1410.3012 [hep-ph].
- [24] ATLAS Collaboration, Measurement of the Z/γ^* boson transverse momentum distribution in pp collisions at $\sqrt{s} = 7$ TeV with the ATLAS detector, *J. High Energy Phys.* 09 (2014) 145, arXiv:1406.3660 [hep-ex].
- [25] J. Pumplin, et al., New generation of parton distributions with uncertainties from global QCD analysis, *J. High Energy Phys.* 07 (2002) 012, arXiv:hep-ph/0201195.
- [26] T. Gleisberg, et al., Event generation with SHERPA 1.1, *J. High Energy Phys.* 02 (2009) 007, arXiv:0811.4622 [hep-ph].
- [27] M. Grazzini, S. Kallweit, D. Rathlev, M. Wiesemann, $W^\pm Z$ production at hadron colliders in NNLO QCD, *Phys. Lett. B* 761 (2016) 179, arXiv:1604.08576 [hep-ph].
- [28] M. Grazzini, S. Kallweit, D. Rathlev, ZZ production at the LHC: fiducial cross sections and distributions in NNLO QCD, *Phys. Lett. B* 750 (2015) 407, arXiv:1507.06257 [hep-ph].
- [29] F. Cascioli, et al., ZZ production at hadron colliders in NNLO QCD, *Phys. Lett. B* 735 (2014) 311, arXiv:1405.2219 [hep-ph].
- [30] E. Bagnaschi, G. Degrandi, P. Slavich, A. Vicini, Higgs production via gluon fusion in the POWHEG approach in the SM and in the MSSM, *J. High Energy Phys.* 02 (2012) 088, arXiv:1111.2854 [hep-ph].
- [31] C. Anastasiou, C. Duhr, F. Dulat, F. Herzog, B. Mistlberger, Higgs boson gluon-fusion production in QCD at three loops, *Phys. Rev. Lett.* 114 (2015) 212001, arXiv:1503.06056 [hep-ph].
- [32] F. Cascioli, et al., Precise Higgs-background predictions: merging NLO QCD and squared quark-loop corrections to four-lepton + 0.1 jet production, *J. High Energy Phys.* 01 (2014) 046, arXiv:1309.0500 [hep-ph].
- [33] F. Caola, K. Melnikov, R. Röntsch, L. Tancredi, QCD corrections to W^+W^- production through gluon fusion, *Phys. Lett. B* 754 (2016) 275, arXiv:1511.08617 [hep-ph].
- [34] J. Alwall, et al., The automated computation of tree-level and next-to-leading order differential cross sections, and their matching to parton shower simulations, *J. High Energy Phys.* 07 (2014) 079, arXiv:1405.0301 [hep-ph].
- [35] NNPDF Collaboration, R.D. Ball, et al., Parton distributions with LHC data, *Nucl. Phys. B* 867 (2013) 244, arXiv:1207.1303 [hep-ph].
- [36] P. Golonka, Z. Was, PHOTOS Monte Carlo: a precision tool for QED corrections in Z and W decays, *Eur. Phys. J. C* 45 (2006) 97, arXiv:hep-ph/0506026.
- [37] C. Anastasiou, L.J. Dixon, K. Melnikov, F. Petriello, High precision QCD at hadron colliders: electroweak gauge boson rapidity distributions at next-to-next-to leading order, *Phys. Rev. D* 69 (2004) 094008, arXiv:hep-ph/0312266.
- [38] J.M. Campbell, R.K. Ellis, P. Nason, E. Re, Top-pair production and decay at NLO matched with parton showers, *J. High Energy Phys.* 04 (2015) 114, arXiv:1412.1828 [hep-ph].
- [39] E. Re, Single-top Wt -channel production matched with parton showers using the POWHEG method, *Eur. Phys. J. C* 71 (2011) 1547, arXiv:1009.2450 [hep-ph].
- [40] T. Sjöstrand, S. Mrenna, P.Z. Skands, PYTHIA 6.4 physics and manual, *J. High Energy Phys.* 05 (2006) 026, arXiv:hep-ph/0603175.
- [41] P.Z. Skands, Tuning Monte Carlo generators: the Perugia tunes, *Phys. Rev. D* 82 (2010) 074018, arXiv:1005.3457 [hep-ph].
- [42] S. Gieseke, et al., Herwig++ 2.5 release note, arXiv:1102.1672 [hep-ph], 2011.
- [43] S. Frixione, E. Laenen, P. Motylinski, B.R. Webber, C.D. White, Single-top hadroproduction in association with a W boson, *J. High Energy Phys.* 07 (2008) 029, arXiv:0805.3067 [hep-ph].
- [44] ATLAS Collaboration, Simulation of top-quark production for the ATLAS experiment at $\sqrt{s} = 13$ TeV, ATL-PHYS-PUB-2016-004, url: <https://cds.cern.ch/record/2120417>, 2016.
- [45] M. Czakon, A. Mitov, Top++: a program for the calculation of the top-pair cross-section at hadron colliders, *Comput. Phys. Commun.* 185 (2014) 2930, arXiv:1112.5675 [hep-ph].
- [46] N. Kidonakis, Two-loop soft anomalous dimensions for single top quark associated production with a W^- or H^- , *Phys. Rev. D* 82 (2010) 054018, arXiv:1005.4451 [hep-ph].
- [47] D.J. Lange, The EvtGen particle decay simulation package, *Nucl. Instrum. Methods A* 462 (2001) 152.
- [48] GEANT4 Collaboration, S. Agostinelli, et al., GEANT4: a simulation toolkit, *Nucl. Instrum. Methods A* 506 (2003) 250.
- [49] ATLAS Collaboration, The ATLAS simulation infrastructure, *Eur. Phys. J. C* 70 (2010) 823, arXiv:1005.4568 [physics.ins-det].
- [50] ATLAS Collaboration, Electron efficiency measurements with the ATLAS detector using the 2015 LHC proton–proton collision data, ATLAS-CONF-2016-024, url: <https://cds.cern.ch/record/2157687>, 2016.
- [51] ATLAS Collaboration, Muon reconstruction performance of the ATLAS detector in proton–proton collision data at $\sqrt{s} = 13$ TeV, *Eur. Phys. J. C* 76 (2016) 292, arXiv:1603.05598 [hep-ex].
- [52] M. Cacciari, G.P. Salam, G. Soyez, The anti- k_t jet clustering algorithm, *J. High Energy Phys.* 04 (2008) 063, arXiv:0802.1189 [hep-ph].
- [53] ATLAS Collaboration, Properties of jets and inputs to jet reconstruction and calibration with the ATLAS detector using proton–proton collisions at $\sqrt{s} = 13$ TeV, ATL-PHYS-PUB-2015-036, url: <https://cds.cern.ch/record/2044564>, 2015.
- [54] ATLAS Collaboration, Jet calibration and systematic uncertainties for jets reconstructed in the ATLAS detector at $\sqrt{s} = 13$ TeV, ATL-PHYS-PUB-2015-015, url: <https://cds.cern.ch/record/2037613>, 2015.
- [55] ATLAS Collaboration, Pile-up subtraction and suppression for jets in ATLAS, ATLAS-CONF-2013-083, url: <https://cds.cern.ch/record/1570994>, 2013.
- [56] ATLAS Collaboration, Tagging and suppression of pileup jets with the ATLAS detector, ATLAS-CONF-2014-018, url: <https://cds.cern.ch/record/1700870>, 2014.
- [57] ATLAS Collaboration, Expected performance of the ATLAS b -tagging algorithms in Run-2, ATL-PHYS-PUB-2015-022, url: <https://cds.cern.ch/record/2037697>, 2015.
- [58] ATLAS Collaboration, Commissioning of the ATLAS b -tagging algorithms using $t\bar{t}$ events in early Run 2 data, ATL-PHYS-PUB-2015-039, url: <https://cds.cern.ch/record/2047871>, 2015.
- [59] ATLAS Collaboration, Expected performance of missing transverse momentum reconstruction for the ATLAS detector at $\sqrt{s} = 13$ TeV, ATL-PHYS-PUB-2015-023, url: <https://cds.cern.ch/record/2037700>, 2015.
- [60] ATLAS Collaboration, Performance of algorithms that reconstruct missing transverse momentum in $\sqrt{s} = 8$ TeV proton–proton collisions in the ATLAS detector, *Eur. Phys. J. C* 77 (2017) 241, arXiv:1609.09324 [hep-ex].
- [61] ATLAS Collaboration, Luminosity determination in pp collisions at $\sqrt{s} = 8$ TeV using the ATLAS detector at the LHC, *Eur. Phys. J. C* 76 (2016) 653, arXiv:1608.03953 [hep-ex].
- [62] J. Wenninger, Energy calibration of the LHC beams at 4 TeV, CERN-ATS-2013-040, url: <https://cds.cern.ch/record/1546734>, 2013.
- [63] MSTW Collaboration, A.D. Martin, et al., Parton distributions for the LHC, *Eur. Phys. J. C* 63 (2009) 189, arXiv:0901.0002 [hep-ph].
- [64] NNPDF Collaboration, R.D. Ball, et al., Parton distributions for the LHC Run II, *J. High Energy Phys.* 04 (2015) 040, arXiv:1410.8849 [hep-ph].
- [65] C. Anastasiou, et al., High precision determination of the gluon fusion Higgs boson cross-section at the LHC, *J. High Energy Phys.* 05 (2016) 058, arXiv:1602.00695 [hep-ph].
- [66] LHC Higgs Cross Section Working Group, Handbook of LHC Higgs cross sections: 4. Deciphering the nature of the Higgs sector, arXiv:1610.07922 [hep-ph], 2016.
- [67] J. Butterworth, et al., PDF4LHC recommendations for LHC Run II, *J. Phys. G* 43 (2016) 023001, arXiv:1510.03865 [hep-ph].
- [68] LHC Higgs Cross Section Working Group, Handbook of LHC Higgs Cross Sections: 3. Higgs properties, arXiv:1307.1347 [hep-ph], 2013.

- [69] ALEPH, DELPHI, L3 and OPAL Collaborations, the LEP Electroweak Working Group, J. Alcaraz, et al., A combination of preliminary electroweak measurements and constraints on the standard model, arXiv:hep-ex/0612034, 2006.
- [70] B. Biedermann, et al., Next-to-leading-order electroweak corrections to $pp \rightarrow W^+W^- \rightarrow 4$ leptons at the LHC, J. High Energy Phys. 06 (2016) 065, arXiv: 1605.03419 [hep-ph].
- [71] I.W. Stewart, F.J. Tackmann, Theory uncertainties for Higgs and other searches using jet bins, Phys. Rev. D 85 (2012) 034011, arXiv:1107.2117 [hep-ph].
- [72] ATLAS Collaboration, ATLAS computing acknowledgements 2016–2017, ATLAS-PUB-2016-002, url: <https://cds.cern.ch/record/2202407>.

The ATLAS Collaboration

M. Aaboud^{137d}, G. Aad⁸⁸, B. Abbott¹¹⁵, J. Abdallah⁸, O. Abdinov¹², B. Abeloos¹¹⁹, R. Aben¹⁰⁹, O.S. AbouZeid¹³⁹, N.L. Abraham¹⁵¹, H. Abramowicz¹⁵⁵, H. Abreu¹⁵⁴, R. Abreu¹¹⁸, Y. Abulaiti^{148a,148b}, B.S. Acharya^{167a,167b,a}, S. Adachi¹⁵⁷, L. Adamczyk^{41a}, D.L. Adams²⁷, J. Adelman¹¹⁰, S. Adomeit¹⁰², T. Adye¹³³, A.A. Affolder⁷⁷, T. Agatonovic-Jovin¹⁴, J.A. Aguilar-Saavedra^{128a,128f}, S.P. Ahlen²⁴, F. Ahmadov^{68,b}, G. Aielli^{135a,135b}, H. Akerstedt^{148a,148b}, T.P.A. Åkesson⁸⁴, A.V. Akimov⁹⁸, G.L. Alberghi^{22a,22b}, J. Albert¹⁷², S. Albrand⁵⁸, M.J. Alconada Verzini⁷⁴, M. Aleksa³², I.N. Aleksandrov⁶⁸, C. Alexa^{28b}, G. Alexander¹⁵⁵, T. Alexopoulos¹⁰, M. Alhroob¹¹⁵, B. Ali¹³⁰, M. Aliev^{76a,76b}, G. Alimonti^{94a}, J. Alison³³, S.P. Alkire³⁸, B.M.M. Allbrooke¹⁵¹, B.W. Allen¹¹⁸, P.P. Allport¹⁹, A. Aloisio^{106a,106b}, A. Alonso³⁹, F. Alonso⁷⁴, C. Alpigiani¹⁴⁰, A.A. Alshehri⁵⁶, M. Alstady⁸⁸, B. Alvarez Gonzalez³², D. Álvarez Piqueras¹⁷⁰, M.G. Alvigi^{106a,106b}, B.T. Amadio¹⁶, Y. Amaral Coutinho^{26a}, C. Amelung²⁵, D. Amidei⁹², S.P. Amor Dos Santos^{128a,128c}, A. Amorim^{128a,128b}, S. Amoroso³², G. Amundsen²⁵, C. Anastopoulos¹⁴¹, L.S. Ancu⁵², N. Andari¹⁹, T. Andeen¹¹, C.F. Anders^{60b}, G. Anders³², J.K. Anders⁷⁷, K.J. Anderson³³, A. Andreazza^{94a,94b}, V. Andrei^{60a}, S. Angelidakis⁹, I. Angelozzi¹⁰⁹, A. Angerami³⁸, F. Anghinolfi³², A.V. Anisenkov^{111,c}, N. Anjos¹³, A. Annovi^{126a,126b}, C. Antel^{60a}, M. Antonelli⁵⁰, A. Antonov^{100,*}, D.J. Antrim¹⁶⁶, F. Anulli^{134a}, M. Aoki⁶⁹, L. Aperio Bella¹⁹, G. Arabidze⁹³, Y. Arai⁶⁹, J.P. Araque^{128a}, A.T.H. Arce⁴⁸, F.A. Arduh⁷⁴, J.-F. Arguin⁹⁷, S. Argyropoulos⁶⁶, M. Arik^{20a}, A.J. Armbruster¹⁴⁵, L.J. Armitage⁷⁹, O. Arnaez³², H. Arnold⁵¹, M. Arratia³⁰, O. Arslan²³, A. Artamonov⁹⁹, G. Artoni¹²², S. Artz⁸⁶, S. Asai¹⁵⁷, N. Asbah⁴⁵, A. Ashkenazi¹⁵⁵, B. Åsman^{148a,148b}, L. Asquith¹⁵¹, K. Assamagan²⁷, R. Astalos^{146a}, M. Atkinson¹⁶⁹, N.B. Atlay¹⁴³, K. Augsten¹³⁰, G. Avolio³², B. Axen¹⁶, M.K. Ayoub¹¹⁹, G. Azuelos^{97,d}, M.A. Baak³², A.E. Baas^{60a}, M.J. Baca¹⁹, H. Bachacou¹³⁸, K. Bachas^{76a,76b}, M. Backes¹²², M. Backhaus³², P. Bagiacchi^{134a,134b}, P. Bagnaia^{134a,134b}, Y. Bai^{35a}, J.T. Baines¹³³, M. Bajic³⁹, O.K. Baker¹⁷⁹, E.M. Baldin^{111,c}, P. Balek¹⁷⁵, T. Balestri¹⁵⁰, F. Balli¹³⁸, W.K. Balunas¹²⁴, E. Banas⁴², Sw. Banerjee^{176,e}, A.A.E. Bannoura¹⁷⁸, L. Barak³², E.L. Barberio⁹¹, D. Barberis^{53a,53b}, M. Barbero⁸⁸, T. Barillari¹⁰³, M.-S. Barisits³², T. Barklow¹⁴⁵, N. Barlow³⁰, S.L. Barnes⁸⁷, B.M. Barnett¹³³, R.M. Barnett¹⁶, Z. Barnovska-Blenessy^{36a}, A. Baroncelli^{136a}, G. Barone²⁵, A.J. Barr¹²², L. Barranco Navarro¹⁷⁰, F. Barreiro⁸⁵, J. Barreiro Guimarães da Costa^{35a}, R. Bartoldus¹⁴⁵, A.E. Barton⁷⁵, P. Bartos^{146a}, A. Basalaev¹²⁵, A. Bassalat^{119,f}, R.L. Bates⁵⁶, S.J. Batista¹⁶¹, J.R. Batley³⁰, M. Battaglia¹³⁹, M. Bause^{134a,134b}, F. Bauer¹³⁸, H.S. Bawa^{145,g}, J.B. Beacham¹¹³, M.D. Beattie⁷⁵, T. Beau⁸³, P.H. Beauchemin¹⁶⁵, P. Bechtel²³, H.P. Beck^{18,h}, K. Becker¹²², M. Becker⁸⁶, M. Beckingham¹⁷³, C. Becot¹¹², A.J. Beddall^{20e}, A. Beddall^{20b}, V.A. Bednyakov⁶⁸, M. Bedognetti¹⁰⁹, C.P. Bee¹⁵⁰, L.J. Beemster¹⁰⁹, T.A. Beermann³², M. Begel²⁷, J.K. Behr⁴⁵, A.S. Bell⁸¹, G. Bella¹⁵⁵, L. Bellagamba^{22a}, A. Bellerive³¹, M. Bellomo⁸⁹, K. Belotskiy¹⁰⁰, O. Beltramello³², N.L. Belyaev¹⁰⁰, O. Benary^{155,*}, D. Benchekroun^{137a}, M. Bender¹⁰², K. Bendtz^{148a,148b}, N. Benekos¹⁰, Y. Benhammou¹⁵⁵, E. Benhar Noccioli¹⁷⁹, J. Benitez⁶⁶, D.P. Benjamin⁴⁸, J.R. Bensinger²⁵, S. Bentvelsen¹⁰⁹, L. Beresford¹²², M. Beretta⁵⁰, D. Berge¹⁰⁹, E. Bergeaas Kuutmann¹⁶⁸, N. Berger⁵, J. Beringer¹⁶, S. Berlendis⁵⁸, N.R. Bernard⁸⁹, C. Bernius¹¹², F.U. Bernlochner²³, T. Berry⁸⁰, P. Berta¹³¹, C. Bertella⁸⁶, G. Bertoli^{148a,148b}, F. Bertolucci^{126a,126b}, I.A. Bertram⁷⁵, C. Bertsche⁴⁵, D. Bertsche¹¹⁵, G.J. Besjes³⁹, O. Bessidskaia Bylund^{148a,148b}, M. Bessner⁴⁵, N. Besson¹³⁸, C. Betancourt⁵¹, A. Bethani⁵⁸, S. Bethke¹⁰³, A.J. Bevan⁷⁹, R.M. Bianchi¹²⁷, M. Bianco³², O. Biebel¹⁰², D. Biedermann¹⁷, R. Bielski⁸⁷, N.V. Biesuz^{126a,126b}, M. Biglietti^{136a}, J. Bilbao De Mendizabal⁵², T.R.V. Billoud⁹⁷, H. Bilokon⁵⁰, M. Bindi⁵⁷, A. Bingul^{20b}, C. Bini^{134a,134b}, S. Biondi^{22a,22b}, T. Bisanz⁵⁷, D.M. Bjergaard⁴⁸, C.W. Black¹⁵², J.E. Black¹⁴⁵, K.M. Black²⁴, D. Blackburn¹⁴⁰, R.E. Blair⁶, T. Blazek^{146a}, I. Bloch⁴⁵, C. Blocker²⁵, A. Blue⁵⁶, W. Blum^{86,*}, U. Blumenschein⁵⁷, S. Blunier^{34a}, G.J. Bobbink¹⁰⁹, V.S. Bobrovnikov^{111,c}, S.S. Bocchetta⁸⁴, A. Bocci⁴⁸, C. Bock¹⁰², M. Boehler⁵¹, D. Boerner¹⁷⁸, J.A. Bogaerts³², D. Bogavac¹⁴, A.G. Bogdanchikov¹¹¹, C. Bohm^{148a}, V. Boisvert⁸⁰, P. Bokan¹⁴, T. Bold^{41a}, A.S. Boldyrev¹⁰¹, M. Bomben⁸³, M. Bona⁷⁹, M. Boonekamp¹³⁸, A. Borisov¹³², G. Borissov⁷⁵, J. Bortfeldt³²,

D. Bortoletto¹²², V. Bortolotto^{62a,62b,62c}, K. Bos¹⁰⁹, D. Boscherini^{22a}, M. Bosman¹³, J.D. Bossio Sola²⁹, J. Boudreau¹²⁷, J. Bouffard², E.V. Bouhova-Thacker⁷⁵, D. Boumediene³⁷, C. Bourdarios¹¹⁹, S.K. Boutle⁵⁶, A. Boveia³², J. Boyd³², I.R. Boyko⁶⁸, J. Bracinik¹⁹, A. Brandt⁸, G. Brandt⁵⁷, O. Brandt^{60a}, U. Bratzler¹⁵⁸, B. Brau⁸⁹, J.E. Brau¹¹⁸, W.D. Breaden Madden⁵⁶, K. Brendlinger¹²⁴, A.J. Brennan⁹¹, L. Brenner¹⁰⁹, R. Brenner¹⁶⁸, S. Bressler¹⁷⁵, T.M. Bristow⁴⁹, D. Britton⁵⁶, D. Britzger⁴⁵, F.M. Brochu³⁰, I. Brock²³, R. Brock⁹³, G. Brooijmans³⁸, T. Brooks⁸⁰, W.K. Brooks^{34b}, J. Brosamer¹⁶, E. Brost¹¹⁰, J.H. Broughton¹⁹, P.A. Bruckman de Renstrom⁴², D. Bruncko^{146b}, R. Bruneliere⁵¹, A. Bruni^{22a}, G. Bruni^{22a}, L.S. Bruni¹⁰⁹, B.H. Brunt³⁰, M. Bruschi^{22a}, N. Bruscino²³, P. Bryant³³, L. Bryngemark⁸⁴, T. Buanes¹⁵, Q. Buat¹⁴⁴, P. Buchholz¹⁴³, A.G. Buckley⁵⁶, I.A. Budagov⁶⁸, F. Buehrer⁵¹, M.K. Bugge¹²¹, O. Bulekov¹⁰⁰, D. Bullock⁸, H. Burckhart³², S. Burdin⁷⁷, C.D. Burgard⁵¹, A.M. Burger⁵, B. Burghgrave¹¹⁰, K. Burka⁴², S. Burke¹³³, I. Burmeister⁴⁶, J.T.P. Burr¹²², E. Busato³⁷, D. Büscher⁵¹, V. Büscher⁸⁶, P. Bussey⁵⁶, J.M. Butler²⁴, C.M. Buttar⁵⁶, J.M. Butterworth⁸¹, P. Butti¹⁰⁹, W. Buttinger²⁷, A. Buzatu⁵⁶, A.R. Buzykaev^{111,c}, S. Cabrera Urbán¹⁷⁰, D. Caforio¹³⁰, V.M. Cairo^{40a,40b}, O. Cakir^{4a}, N. Calace⁵², P. Calafiura¹⁶, A. Calandri⁸⁸, G. Calderini⁸³, P. Calfayan⁶⁴, G. Callea^{40a,40b}, L.P. Caloba^{26a}, S. Calvente Lopez⁸⁵, D. Calvet³⁷, S. Calvet³⁷, T.P. Calvet⁸⁸, R. Camacho Toro³³, S. Camarda³², P. Camarri^{135a,135b}, D. Cameron¹²¹, R. Caminal Armadans¹⁶⁹, C. Camincher⁵⁸, S. Campana³², M. Campanelli⁸¹, A. Camplani^{94a,94b}, A. Campoverde¹⁴³, V. Canale^{106a,106b}, A. Canepa^{163a}, M. Cano Bret^{36c}, J. Cantero¹¹⁶, T. Cao¹⁵⁵, M.D.M. Capeans Garrido³², I. Caprini^{28b}, M. Caprini^{28b}, M. Capua^{40a,40b}, R.M. Carbone³⁸, R. Cardarelli^{135a}, F. Cardillo⁵¹, I. Carli¹³¹, T. Carli³², G. Carlino^{106a}, L. Carminati^{94a,94b}, R.M.D. Carney^{148a,148b}, S. Caron¹⁰⁸, E. Carquin^{34b}, G.D. Carrillo-Montoya³², J.R. Carter³⁰, J. Carvalho^{128a,128c}, D. Casadei¹⁹, M.P. Casado^{13,i}, M. Casolino¹³, D.W. Casper¹⁶⁶, E. Castaneda-Miranda^{147a}, R. Castelijns¹⁰⁹, A. Castelli¹⁰⁹, V. Castillo Gimenez¹⁷⁰, N.F. Castro^{128a,j}, A. Catinaccio³², J.R. Catmore¹²¹, A. Cattai³², J. Caudron²³, V. Cavaliere¹⁶⁹, E. Cavallaro¹³, D. Cavalli^{94a}, M. Cavalli-Sforza¹³, V. Cavasinni^{126a,126b}, F. Ceradini^{136a,136b}, L. Cerda Alberich¹⁷⁰, A.S. Cerqueira^{26b}, A. Cerri¹⁵¹, L. Cerrito^{135a,135b}, F. Cerutti¹⁶, A. Cervelli¹⁸, S.A. Cetin^{20d}, A. Chafaq^{137a}, D. Chakraborty¹¹⁰, S.K. Chan⁵⁹, Y.L. Chan^{62a}, P. Chang¹⁶⁹, J.D. Chapman³⁰, D.G. Charlton¹⁹, A. Chatterjee⁵², C.C. Chau¹⁶¹, C.A. Chavez Barajas¹⁵¹, S. Che¹¹³, S. Cheatham^{167a,167c}, A. Chegwiddden⁹³, S. Chekanov⁶, S.V. Chekulaev^{163a}, G.A. Chelkov^{68,k}, M.A. Chelstowska⁹², C. Chen⁶⁷, H. Chen²⁷, K. Chen¹⁵⁰, S. Chen^{35b}, S. Chen¹⁵⁷, X. Chen^{35c}, Y. Chen⁷⁰, H.C. Cheng⁹², H.J. Cheng^{35a}, Y. Cheng³³, A. Cheplakov⁶⁸, E. Cheremushkina¹³², R. Cherkaoui El Moursli^{137e}, V. Chernyatin^{27,*}, E. Cheu⁷, L. Chevalier¹³⁸, V. Chiarella⁵⁰, G. Chiarelli^{126a,126b}, G. Chiodini^{76a}, A.S. Chisholm³², A. Chitan^{28b}, M.V. Chizhov⁶⁸, K. Choi⁶⁴, A.R. Chomont³⁷, S. Chouridou⁹, B.K.B. Chow¹⁰², V. Christodoulou⁸¹, D. Chromek-Burckhart³², J. Chudoba¹²⁹, A.J. Chuinard⁹⁰, J.J. Chwastowski⁴², L. Chytka¹¹⁷, G. Ciapetti^{134a,134b}, A.K. Ciftci^{4a}, D. Cinca⁴⁶, V. Cindro⁷⁸, I.A. Cioara²³, C. Ciocca^{22a,22b}, A. Ciochio¹⁶, F. Ciotto^{106a,106b}, Z.H. Citron¹⁷⁵, M. Citterio^{94a}, M. Ciubancan^{28b}, A. Clark⁵², B.L. Clark⁵⁹, M.R. Clark³⁸, P.J. Clark⁴⁹, R.N. Clarke¹⁶, C. Clement^{148a,148b}, Y. Coadou⁸⁸, M. Cobl^{167a,167c}, A. Coccaro⁵², J. Cochran⁶⁷, L. Colasurdo¹⁰⁸, B. Cole³⁸, A.P. Colijn¹⁰⁹, J. Collot⁵⁸, T. Colombo¹⁶⁶, G. Compostella¹⁰³, P. Conde Muiño^{128a,128b}, E. Coniavitis⁵¹, S.H. Connell^{147b}, I.A. Connelly⁸⁰, V. Consorti⁵¹, S. Constantinescu^{28b}, G. Conti³², F. Conventi^{106a,l}, M. Cooke¹⁶, B.D. Cooper⁸¹, A.M. Cooper-Sarkar¹²², F. Cormier¹⁷¹, K.J.R. Cormier¹⁶¹, T. Cornelissen¹⁷⁸, M. Corradi^{134a,134b}, F. Corriveau^{90,m}, A. Cortes-Gonzalez³², G. Cortiana¹⁰³, G. Costa^{94a}, M.J. Costa¹⁷⁰, D. Costanzo¹⁴¹, G. Cottin³⁰, G. Cowan⁸⁰, B.E. Cox⁸⁷, K. Cranmer¹¹², S.J. Crawley⁵⁶, G. Cree³¹, S. Crépé-Renaudin⁵⁸, F. Crescioli⁸³, W.A. Cribbs^{148a,148b}, M. Crispin Ortuzar¹²², M. Cristinziani²³, V. Croft¹⁰⁸, G. Crosetti^{40a,40b}, A. Cueto⁸⁵, T. Cuhadar Donszelmann¹⁴¹, J. Cummings¹⁷⁹, M. Curatolo⁵⁰, J. Cúth⁸⁶, H. Czirr¹⁴³, P. Czodrowski³, G. D'amen^{22a,22b}, S. D'Auria⁵⁶, M. D'Onofrio⁷⁷, M.J. Da Cunha Sargedass De Sousa^{128a,128b}, C. Da Via⁸⁷, W. Dabrowski^{41a}, T. Dado^{146a}, T. Dai⁹², O. Dale¹⁵, F. Dallaire⁹⁷, C. Dallapiccola⁸⁹, M. Dam³⁹, J.R. Dandoy³³, N.P. Dang⁵¹, A.C. Daniells¹⁹, N.S. Dann⁸⁷, M. Danninger¹⁷¹, M. Dano Hoffmann¹³⁸, V. Dao⁵¹, G. Darbo^{53a}, S. Darmora⁸, J. Dassoulas³, A. Dattagupta¹¹⁸, W. Davey²³, C. David¹⁷², T. Davidek¹³¹, M. Davies¹⁵⁵, P. Davison⁸¹, E. Dawe⁹¹, I. Dawson¹⁴¹, K. De⁸, R. de Asmundis^{106a}, A. De Benedetti¹¹⁵, S. De Castro^{22a,22b}, S. De Cecco⁸³, N. De Groot¹⁰⁸, P. de Jong¹⁰⁹, H. De la Torre⁹³, F. De Lorenzi⁶⁷, A. De Maria⁵⁷, D. De Pedis^{134a}, A. De Salvo^{134a}, U. De Sanctis¹⁵¹, A. De Santo¹⁵¹, J.B. De Vivie De Regie¹¹⁹, W.J. Dearnaley⁷⁵, R. Debbe²⁷, C. Debenedetti¹³⁹, D.V. Dedovich⁶⁸,

N. Dehghanian³, I. Deigaard¹⁰⁹, M. Del Gaudio^{40a,40b}, J. Del Peso⁸⁵, T. Del Prete^{126a,126b}, D. Delgove¹¹⁹, F. Deliot¹³⁸, C.M. Delitzsch⁵², A. Dell'Acqua³², L. Dell'Asta²⁴, M. Dell'Orso^{126a,126b}, M. Della Pietra^{106a,l}, D. della Volpe⁵², M. Delmastro⁵, P.A. Delsart⁵⁸, D.A. DeMarco¹⁶¹, S. Demers¹⁷⁹, M. Demichev⁶⁸, A. Demilly⁸³, S.P. Denisov¹³², D. Denysiuk¹³⁸, D. Derendarz⁴², J.E. Derkaoui^{137d}, F. Derue⁸³, P. Dervan⁷⁷, K. Desch²³, C. Deterre⁴⁵, K. Dette⁴⁶, P.O. Deviveiros³², A. Dewhurst¹³³, S. Dhaliwal²⁵, A. Di Ciaccio^{135a,135b}, L. Di Ciaccio⁵, W.K. Di Clemente¹²⁴, C. Di Donato^{106a,106b}, A. Di Girolamo³², B. Di Girolamo³², B. Di Micco^{136a,136b}, R. Di Nardo³², A. Di Simone⁵¹, R. Di Sipio¹⁶¹, D. Di Valentino³¹, C. Diaconu⁸⁸, M. Diamond¹⁶¹, F.A. Dias⁴⁹, M.A. Diaz^{34a}, E.B. Diehl⁹², J. Dietrich¹⁷, S. Díez Cornell⁴⁵, A. Dimitrievska¹⁴, J. Dingfelder²³, P. Dita^{28b}, S. Dita^{28b}, F. Dittus³², F. Djama⁸⁸, T. Djobava^{54b}, J.I. Djuvsland^{60a}, M.A.B. do Vale^{26c}, D. Dobos³², M. Dobre^{28b}, C. Doglioni⁸⁴, J. Dolejsi¹³¹, Z. Dolezal¹³¹, M. Donadelli^{26d}, S. Donati^{126a,126b}, P. Dondero^{123a,123b}, J. Donini³⁷, J. Dopke¹³³, A. Doria^{106a}, M.T. Dova⁷⁴, A.T. Doyle⁵⁶, E. Drechsler⁵⁷, M. Dris¹⁰, Y. Du^{36b}, J. Duarte-Campderros¹⁵⁵, E. Duchovni¹⁷⁵, G. Duckeck¹⁰², O.A. Ducu^{97,n}, D. Duda¹⁰⁹, A. Dudarev³², A. Chr. Dudder⁸⁶, E.M. Duffield¹⁶, L. Duflot¹¹⁹, M. Dührssen³², M. Dumancic¹⁷⁵, A.K. Duncan⁵⁶, M. Dunford^{60a}, H. Duran Yildiz^{4a}, M. Düren⁵⁵, A. Durglischvili^{54b}, D. Duschinger⁴⁷, B. Dutta⁴⁵, M. Dyndal⁴⁵, C. Eckardt⁴⁵, K.M. Ecker¹⁰³, R.C. Edgar⁹², N.C. Edwards⁴⁹, T. Eifert³², G. Eigen¹⁵, K. Einsweiler¹⁶, T. Ekelof¹⁶⁸, M. El Kacimi^{137c}, V. Ellajosyula⁸⁸, M. Ellert¹⁶⁸, S. Elles⁵, F. Ellinghaus¹⁷⁸, A.A. Elliot¹⁷², N. Ellis³², J. Elmsheuser²⁷, M. Elsing³², D. Emeliyanov¹³³, Y. Enari¹⁵⁷, O.C. Endner⁸⁶, J.S. Ennis¹⁷³, J. Erdmann⁴⁶, A. Ereditato¹⁸, G. Ernis¹⁷⁸, J. Ernst², M. Ernst²⁷, S. Errede¹⁶⁹, E. Ertel⁸⁶, M. Escalier¹¹⁹, H. Esch⁴⁶, C. Escobar¹²⁷, B. Esposito⁵⁰, A.I. Etienvre¹³⁸, E. Etzion¹⁵⁵, H. Evans⁶⁴, A. Ezhilov¹²⁵, M. Ezzi^{137e}, F. Fabbri^{22a,22b}, L. Fabbri^{22a,22b}, G. Facini³³, R.M. Fakhruddinov¹³², S. Falciano^{134a}, R.J. Falla⁸¹, J. Faltova³², Y. Fang^{35a}, M. Fanti^{94a,94b}, A. Farbin⁸, A. Farilla^{136a}, C. Farina¹²⁷, E.M. Farina^{123a,123b}, T. Farooque¹³, S. Farrell¹⁶, S.M. Farrington¹⁷³, P. Farthouat³², F. Fassi^{137e}, P. Fassnacht³², D. Fassoulitis⁹, M. Faucci Giannelli⁸⁰, A. Favareto^{53a,53b}, W.J. Fawcett¹²², L. Fayard¹¹⁹, O.L. Fedin^{125,o}, W. Fedorko¹⁷¹, S. Feigl¹²¹, L. Feligioni⁸⁸, C. Feng^{36b}, E.J. Feng³², H. Feng⁹², A.B. Fenyuk¹³², L. Feremenga⁸, P. Fernandez Martinez¹⁷⁰, S. Fernandez Perez¹³, J. Ferrando⁴⁵, A. Ferrari¹⁶⁸, P. Ferrari¹⁰⁹, R. Ferrari^{123a}, D.E. Ferreira de Lima^{60b}, A. Ferrer¹⁷⁰, D. Ferrere⁵², C. Ferretti⁹², F. Fiedler⁸⁶, A. Filipčič⁷⁸, M. Filipuzzi⁴⁵, F. Filthaut¹⁰⁸, M. Fincke-Keeler¹⁷², K.D. Finelli¹⁵², M.C.N. Fiolhais^{128a,128c}, L. Fiorini¹⁷⁰, A. Fischer², C. Fischer¹³, J. Fischer¹⁷⁸, W.C. Fisher⁹³, N. Flaschel⁴⁵, I. Fleck¹⁴³, P. Fleischmann⁹², G.T. Fletcher¹⁴¹, R.R.M. Fletcher¹²⁴, T. Flick¹⁷⁸, B.M. Flierl¹⁰², L.R. Flores Castillo^{62a}, M.J. Flowerdew¹⁰³, G.T. Forcolin⁸⁷, A. Formica¹³⁸, A. Forti⁸⁷, A.G. Foster¹⁹, D. Fournier¹¹⁹, H. Fox⁷⁵, S. Fracchia¹³, P. Francavilla⁸³, M. Franchini^{22a,22b}, D. Francis³², L. Franconi¹²¹, M. Franklin⁵⁹, M. Frate¹⁶⁶, M. Fraternali^{123a,123b}, D. Freeborn⁸¹, S.M. Fressard-Batraneanu³², F. Friedrich⁴⁷, D. Froidevaux³², J.A. Frost¹²², C. Fukunaga¹⁵⁸, E. Fullana Torregrosa⁸⁶, T. Fusayas¹⁰⁴, J. Fuster¹⁷⁰, C. Gabaldon⁵⁸, O. Gabizon¹⁵⁴, A. Gabrielli^{22a,22b}, A. Gabrielli¹⁶, G.P. Gach^{41a}, S. Gadatsch³², G. Gagliardi^{53a,53b}, L.G. Gagnon⁹⁷, P. Gagnon⁶⁴, C. Galea¹⁰⁸, B. Galhardo^{128a,128c}, E.J. Gallas¹²², B.J. Gallop¹³³, P. Gallus¹³⁰, G. Galster³⁹, K.K. Gan¹¹³, S. Ganguly³⁷, J. Gao^{36a}, Y. Gao⁴⁹, Y.S. Gao^{145,g}, F.M. Garay Walls⁴⁹, C. García¹⁷⁰, J.E. García Navarro¹⁷⁰, M. Garcia-Sciveres¹⁶, R.W. Gardner³³, N. Garelli¹⁴⁵, V. Garonne¹²¹, A. Gascon Bravo⁴⁵, K. Gasnikova⁴⁵, C. Gatti⁵⁰, A. Gaudiello^{53a,53b}, G. Gaudio^{123a}, L. Gauthier⁹⁷, I.L. Gavrilenko⁹⁸, C. Gay¹⁷¹, G. Gaycken²³, E.N. Gazis¹⁰, Z. Gece¹⁷¹, C.N.P. Gee¹³³, Ch. Geich-Gimbel²³, M. Geisen⁸⁶, M.P. Geisler^{60a}, K. Gellerstedt^{148a,148b}, C. Gemme^{53a}, M.H. Genest⁵⁸, C. Geng^{36a,p}, S. Gentile^{134a,134b}, C. Gentsos¹⁵⁶, S. George⁸⁰, D. Gerbaudo¹³, A. Gershon¹⁵⁵, S. Ghasemi¹⁴³, M. Ghneimat²³, B. Giacobbe^{22a}, S. Giagu^{134a,134b}, P. Giannetti^{126a,126b}, S.M. Gibson⁸⁰, M. Gignac¹⁷¹, M. Gilchriese¹⁶, T.P.S. Gillam³⁰, D. Gillberg³¹, G. Gilles¹⁷⁸, D.M. Gingrich^{3,d}, N. Giokaris^{9,*}, M.P. Giordani^{167a,167c}, F.M. Giorgi^{22a}, P.F. Giraud¹³⁸, P. Giromini⁵⁹, D. Giugni^{94a}, F. Giuli¹²², C. Giuliani¹⁰³, M. Giulini^{60b}, B.K. Gjelsten¹²¹, S. Gkaitatzis¹⁵⁶, I. Gkialas¹⁵⁶, E.L. Gkougkousis¹¹⁹, L.K. Gladilin¹⁰¹, C. Glasman⁸⁵, J. Glatzer¹³, P.C.F. Glaysher⁴⁹, A. Glazov⁴⁵, M. Goblirsch-Kolb²⁵, J. Godlewski⁴², S. Goldfarb⁹¹, T. Golling⁵², D. Golubkov¹³², A. Gomes^{128a,128b,128d}, R. Gonçalves^{128a}, J. Goncalves Pinto Firmino Da Costa¹³⁸, G. Gonella⁵¹, L. Gonella¹⁹, A. Gongadze⁶⁸, S. González de la Hoz¹⁷⁰, S. Gonzalez-Sevilla⁵², L. Goossens³², P.A. Gorbounov⁹⁹, H.A. Gordon²⁷, I. Gorelov¹⁰⁷, B. Gorini³², E. Gorini^{76a,76b}, A. Gorišek⁷⁸, E. Gornicki⁴², A.T. Goshaw⁴⁸, C. Gössling⁴⁶, M.I. Gostkin⁶⁸, C.R. Goudet¹¹⁹, D. Goujdami^{137c}, A.G. Goussiou¹⁴⁰, N. Govender^{147b,q}, E. Gozani¹⁵⁴,

L. Graber⁵⁷, I. Grabowska-Bold^{41a}, P.O.J. Gradin⁵⁸, P. Grafström^{22a,22b}, J. Gramling⁵², E. Gramstad¹²¹, S. Grancagnolo¹⁷, V. Gratchev¹²⁵, P.M. Gravila^{28e}, H.M. Gray³², E. Graziani^{136a}, Z.D. Greenwood^{82,r}, C. Greife²³, K. Gregersen⁸¹, I.M. Gregor⁴⁵, P. Grenier¹⁴⁵, K. Grevtsov⁵, J. Griffiths⁸, A.A. Grillo¹³⁹, K. Grimm⁷⁵, S. Grinstein^{13,s}, Ph. Gris³⁷, J.-F. Grivaz¹¹⁹, S. Groh⁸⁶, E. Gross¹⁷⁵, J. Grosse-Knetter⁵⁷, G.C. Grossi⁸², Z.J. Grout⁸¹, L. Guan⁹², W. Guan¹⁷⁶, J. Guenther⁶⁵, F. Guescini⁵², D. Guest¹⁶⁶, O. Gueta¹⁵⁵, B. Gui¹¹³, E. Guido^{53a,53b}, T. Guillemin⁵, S. Guindon², U. Gul⁵⁶, C. Gumpert³², J. Guo^{36c}, Y. Guo^{36a,p}, R. Gupta⁴³, S. Gupta¹²², G. Gustavino^{134a,134b}, P. Gutierrez¹¹⁵, N.G. Gutierrez Ortiz⁸¹, C. Gutsche⁸¹, C. Guyot¹³⁸, C. Gwenlan¹²², C.B. Gwilliam⁷⁷, A. Haas¹¹², C. Haber¹⁶, H.K. Hadavand⁸, N. Haddad^{137e}, A. Hadeef⁸⁸, S. Hageböck²³, M. Hagihara¹⁶⁴, Z. Hajduk⁴², H. Hakobyan^{180,*}, M. Haleem⁴⁵, J. Haley¹¹⁶, G. Halladjian⁹³, G.D. Hallewell⁸⁸, K. Hamacher¹⁷⁸, P. Hamal¹¹⁷, K. Hamano¹⁷², A. Hamilton^{147a}, G.N. Hamity¹⁴¹, P.G. Hamnett⁴⁵, L. Han^{36a}, K. Hanagaki^{69,t}, K. Hanawa¹⁵⁷, M. Hance¹³⁹, B. Haney¹²⁴, P. Hanke^{60a}, R. Hanna¹³⁸, J.B. Hansen³⁹, J.D. Hansen³⁹, M.C. Hansen²³, P.H. Hansen³⁹, K. Hara¹⁶⁴, A.S. Hard¹⁷⁶, T. Harenberg¹⁷⁸, F. Hariri¹¹⁹, S. Harkusha⁹⁵, R.D. Harrington⁴⁹, P.F. Harrison¹⁷³, F. Hartjes¹⁰⁹, N.M. Hartmann¹⁰², M. Hasegawa⁷⁰, Y. Hasegawa¹⁴², A. Hasib¹¹⁵, S. Hassani¹³⁸, S. Haug¹⁸, R. Hauser⁹³, L. Hauswald⁴⁷, M. Havranek¹²⁹, C.M. Hawkes¹⁹, R.J. Hawking³², D. Hayakawa¹⁵⁹, D. Hayden⁹³, C.P. Hays¹²², J.M. Hays⁷⁹, H.S. Hayward⁷⁷, S.J. Haywood¹³³, S.J. Head¹⁹, T. Heck⁸⁶, V. Hedberg⁸⁴, L. Heelan⁸, S. Heim¹²⁴, T. Heim¹⁶, B. Heinemann¹⁶, J.J. Heinrich¹⁰², L. Heinrich¹¹², C. Heinz⁵⁵, J. Hejbal¹²⁹, L. Helary³², S. Hellman^{148a,148b}, C. Hensens³², J. Henderson¹²², R.C.W. Henderson⁷⁵, Y. Heng¹⁷⁶, S. Henkelmann¹⁷¹, A.M. Henriques Correia³², S. Henrot-Versille¹¹⁹, G.H. Herbert¹⁷, H. Herde²⁵, V. Herget¹⁷⁷, Y. Hernández Jiménez^{147c}, G. Herten⁵¹, R. Hertenberger¹⁰², L. Hervas³², G.G. Hesketh⁸¹, N.P. Hessey¹⁰⁹, J.W. Hetherly⁴³, E. Higón-Rodríguez¹⁷⁰, E. Hill¹⁷², J.C. Hill³⁰, K.H. Hiller⁴⁵, S.J. Hillier¹⁹, I. Hinchliffe¹⁶, E. Hines¹²⁴, R.R. Hinman¹⁶, M. Hirose⁵¹, D. Hirschbuehl¹⁷⁸, X. Hoad⁴⁹, J. Hobbs¹⁵⁰, N. Hod^{163a}, M.C. Hodgkinson¹⁴¹, P. Hodgson¹⁴¹, A. Hoecker³², M.R. Hoferkamp¹⁰⁷, F. Hoenig¹⁰², D. Hohn²³, T.R. Holmes¹⁶, M. Homann⁴⁶, T. Honda⁶⁹, T.M. Hong¹²⁷, B.H. Hooberman¹⁶⁹, W.H. Hopkins¹¹⁸, Y. Horii¹⁰⁵, A.J. Horton¹⁴⁴, J.-Y. Hostachy⁵⁸, S. Hou¹⁵³, A. Hoummada^{137a}, J. Howarth⁴⁵, J. Hoya⁷⁴, M. Hrabovsky¹¹⁷, I. Hristova¹⁷, J. Hrivnac¹¹⁹, T. Hryn'ova⁵, A. Hrynevich⁹⁶, P.J. Hsu⁶³, S.-C. Hsu¹⁴⁰, Q. Hu^{36a}, S. Hu^{36c}, Y. Huang⁴⁵, Z. Hubacek¹³⁰, F. Hubaut⁸⁸, F. Huegging²³, T.B. Huffman¹²², E.W. Hughes³⁸, G. Hughes⁷⁵, M. Huhtinen³², P. Huo¹⁵⁰, N. Huseynov^{68,b}, J. Huston⁹³, J. Huth⁵⁹, G. Iacobucci⁵², G. Iakovidis²⁷, I. Ibragimov¹⁴³, L. Iconomidou-Fayard¹¹⁹, E. Ideal¹⁷⁹, Z. Idrissi^{137e}, P. Iengo³², O. Igonkina^{109,u}, T. Iizawa¹⁷⁴, Y. Ikegami⁶⁹, M. Ikeno⁶⁹, Y. Ilchenko^{11,v}, D. Iliadis¹⁵⁶, N. Ilic¹⁴⁵, G. Introzzi^{123a,123b}, P. Ioannou^{9,*}, M. Iodice^{136a}, K. Iordanidou³⁸, V. Ippolito⁵⁹, N. Ishijima¹²⁰, M. Ishino¹⁵⁷, M. Ishitsuka¹⁵⁹, R. Ishmukhametov¹¹³, C. Issever¹²², S. Istin^{20a}, F. Ito¹⁶⁴, J.M. Iturbe Ponce⁸⁷, R. Iuppa^{162a,162b}, W. Iwanski⁶⁵, H. Iwasaki⁶⁹, J.M. Izen⁴⁴, V. Izzo^{106a}, S. Jabbar³, B. Jackson¹²⁴, P. Jackson¹, V. Jain², K.B. Jakobi⁸⁶, K. Jakobs⁵¹, S. Jakobsen³², T. Jakoubek¹²⁹, D.O. Jamin¹¹⁶, D.K. Jana⁸², R. Jansky⁶⁵, J. Janssen²³, M. Janus⁵⁷, P.A. Janus^{41a}, G. Jarlskog⁸⁴, N. Javadov^{68,b}, T. Javůrek⁵¹, M. Javurkova⁵¹, F. Jeanneau¹³⁸, L. Jeanty¹⁶, J. Jejelava^{54a,w}, G.-Y. Jeng¹⁵², D. Jennens⁹¹, P. Jenni^{51,x}, C. Jeske¹⁷³, S. Jézéquel⁵, H. Ji¹⁷⁶, J. Jia¹⁵⁰, H. Jiang⁶⁷, Y. Jiang^{36a}, Z. Jiang¹⁴⁵, S. Jiggins⁸¹, J. Jimenez Pena¹⁷⁰, S. Jin^{35a}, A. Jinaru^{28b}, O. Jinnouchi¹⁵⁹, H. Jivan^{147c}, P. Johansson¹⁴¹, K.A. Johns⁷, W.J. Johnson¹⁴⁰, K. Jon-And^{148a,148b}, G. Jones¹⁷³, R.W.L. Jones⁷⁵, S. Jones⁷, T.J. Jones⁷⁷, J. Jongmanns^{60a}, P.M. Jorge^{128a,128b}, J. Jovicevic^{163a}, X. Ju¹⁷⁶, A. Juste Rozas^{13,s}, M.K. Köhler¹⁷⁵, A. Kaczmarska⁴², M. Kado¹¹⁹, H. Kagan¹¹³, M. Kagan¹⁴⁵, S.J. Kahn⁸⁸, T. Kaji¹⁷⁴, E. Kajomovitz⁴⁸, C.W. Kalderon¹²², A. Kaluza⁸⁶, S. Kama⁴³, A. Kamenshchikov¹³², N. Kanaya¹⁵⁷, S. Kaneti³⁰, L. Kanjir⁷⁸, V.A. Kantserov¹⁰⁰, J. Kanzaki⁶⁹, B. Kaplan¹¹², L.S. Kaplan¹⁷⁶, A. Kapliy³³, D. Kar^{147c}, K. Karakostas¹⁰, A. Karamaoun³, N. Karastathis¹⁰, M.J. Kareem⁵⁷, E. Karentzos¹⁰, M. Karnevskiy⁸⁶, S.N. Karpov⁶⁸, Z.M. Karpova⁶⁸, K. Karthik¹¹², V. Kartvelishvili⁷⁵, A.N. Karyukhin¹³², K. Kasahara¹⁶⁴, L. Kashif¹⁷⁶, R.D. Kass¹¹³, A. Kastanas¹⁴⁹, Y. Kataoka¹⁵⁷, C. Kato¹⁵⁷, A. Katre⁵², J. Katzy⁴⁵, K. Kawade¹⁰⁵, K. Kawagoe⁷³, T. Kawamoto¹⁵⁷, G. Kawamura⁵⁷, V.F. Kazanin^{111,c}, R. Keeler¹⁷², R. Kehoe⁴³, J.S. Keller⁴⁵, J.J. Kempster⁸⁰, H. Keoshkerian¹⁶¹, O. Kepka¹²⁹, B.P. Kerševan⁷⁸, S. Kersten¹⁷⁸, R.A. Keyes⁹⁰, M. Khader¹⁶⁹, F. Khalil-zada¹², A. Khanov¹¹⁶, A.G. Kharlamov^{111,c}, T. Kharlamova^{111,c}, T.J. Khoo⁵², V. Khovanskiy⁹⁹, E. Khramov⁶⁸, J. Khubua^{54b,y}, S. Kido⁷⁰, C.R. Kilby⁸⁰, H.Y. Kim⁸, S.H. Kim¹⁶⁴, Y.K. Kim³³, N. Kimura¹⁵⁶, O.M. Kind¹⁷, B.T. King⁷⁷, M. King¹⁷⁰, J. Kirk¹³³, A.E. Kiryunin¹⁰³,

T. Kishimoto¹⁵⁷, D. Kisielewska^{41a}, F. Kiss⁵¹, K. Kiuchi¹⁶⁴, O. Kivernyk¹³⁸, E. Kladiva^{146b}, M.H. Klein³⁸, M. Klein⁷⁷, U. Klein⁷⁷, K. Kleinknecht⁸⁶, P. Klimek¹¹⁰, A. Klimentov²⁷, R. Klingenberg⁴⁶, T. Klioutchnikova³², E.-E. Kluge^{60a}, P. Kluit¹⁰⁹, S. Kluth¹⁰³, J. Knapik⁴², E. Kneringer⁶⁵, E.B.F.G. Knoop⁸⁸, A. Knue¹⁰³, A. Kobayashi¹⁵⁷, D. Kobayashi¹⁵⁹, T. Kobayashi¹⁵⁷, M. Kobel⁴⁷, M. Kocian¹⁴⁵, P. Kodys¹³¹, T. Koffas³¹, E. Koffeman¹⁰⁹, N.M. Köhler¹⁰³, T. Koi¹⁴⁵, H. Kolanoski¹⁷, M. Kolb^{60b}, I. Koletsou⁵, A.A. Komar^{98,*}, Y. Komori¹⁵⁷, T. Kondo⁶⁹, N. Kondrashova^{36c}, K. Köneke⁵¹, A.C. König¹⁰⁸, T. Kono^{69,z}, R. Konoplich^{112,aa}, N. Konstantinidis⁸¹, R. Kopeliansky⁶⁴, S. Koperny^{41a}, L. Köpke⁸⁶, A.K. Kopp⁵¹, K. Korcyl⁴², K. Kordas¹⁵⁶, A. Korn⁸¹, A.A. Korol^{111,c}, I. Korolkov¹³, E.V. Korolkova¹⁴¹, O. Kortner¹⁰³, S. Kortner¹⁰³, T. Kosek¹³¹, V.V. Kostyukhin²³, A. Kotwal⁴⁸, A. Koulouris¹⁰, A. Kourkumeli-Charalampidi^{123a,123b}, C. Kourkumelis⁹, V. Kouskoura²⁷, A.B. Kowalewska⁴², R. Kowalewski¹⁷², T.Z. Kowalski^{41a}, C. Kozakai¹⁵⁷, W. Kozanecki¹³⁸, A.S. Kozhin¹³², V.A. Kramarenko¹⁰¹, G. Kramberger⁷⁸, D. Krasnopevtsev¹⁰⁰, M.W. Krasny⁸³, A. Krasznahorkay³², A. Kravchenko²⁷, M. Kretz^{60c}, J. Kretzschmar⁷⁷, K. Kreutzfeldt⁵⁵, P. Krieger¹⁶¹, K. Krizka³³, K. Kroeninger⁴⁶, H. Kroha¹⁰³, J. Kroll¹²⁴, J. Kroseberg²³, J. Krstic¹⁴, U. Kruchonak⁶⁸, H. Krüger²³, N. Krumnack⁶⁷, M.C. Kruse⁴⁸, M. Kruskal²⁴, T. Kubota⁹¹, H. Kucuk⁸¹, S. Kuday^{4b}, J.T. Kuechler¹⁷⁸, S. Kuehn⁵¹, A. Kugel^{60c}, F. Kuger¹⁷⁷, T. Kuhl⁴⁵, V. Kukhtin⁶⁸, R. Kukla¹³⁸, Y. Kulchitsky⁹⁵, S. Kuleshov^{34b}, M. Kuna^{134a,134b}, T. Kunigo⁷¹, A. Kupco¹²⁹, H. Kurashige⁷⁰, L.L. Kurchaninov^{163a}, Y.A. Kurochkin⁹⁵, M.G. Kurth⁴⁴, V. Kus¹²⁹, E.S. Kuwertz¹⁷², M. Kuze¹⁵⁹, J. Kvita¹¹⁷, T. Kwan¹⁷², D. Kyriazopoulos¹⁴¹, A. La Rosa¹⁰³, J.L. La Rosa Navarro^{26d}, L. La Rotonda^{40a,40b}, C. Lacasta¹⁷⁰, F. Lacava^{134a,134b}, J. Lacey³¹, H. Lacker¹⁷, D. Lacour⁸³, V.R. Lacuesta¹⁷⁰, E. Ladygin⁶⁸, R. Lafaye⁵, B. Laforge⁸³, T. Lagouri¹⁷⁹, S. Lai⁵⁷, S. Lammers⁶⁴, W. Lampl⁷, E. Lançon¹³⁸, U. Landgraf⁵¹, M.P.J. Landon⁷⁹, M.C. Lanfermann⁵², V.S. Lang^{60a}, J.C. Lange¹³, A.J. Lankford¹⁶⁶, F. Lanni²⁷, K. Lantzsch²³, A. Lanza^{123a}, S. Laplace⁸³, C. Lapoire³², J.F. Laporte¹³⁸, T. Lari^{94a}, F. Lasagni Manghi^{22a,22b}, M. Lassnig³², P. Laurelli⁵⁰, W. Lavrijsen¹⁶, A.T. Law¹³⁹, P. Laycock⁷⁷, T. Lazovich⁵⁹, M. Lazzaroni^{94a,94b}, B. Le⁹¹, O. Le Dortz⁸³, E. Le Guirriec⁸⁸, E.P. Le Quilleuc¹³⁸, M. LeBlanc¹⁷², T. LeCompte⁶, F. Ledroit-Guillon⁵⁸, C.A. Lee²⁷, S.C. Lee¹⁵³, L. Lee¹, B. Lefebvre⁹⁰, G. Lefebvre⁸³, M. Lefebvre¹⁷², F. Legger¹⁰², C. Leggett¹⁶, A. Lehan⁷⁷, G. Lehmann Miotto³², X. Lei⁷, W.A. Leight³¹, A.G. Leister¹⁷⁹, M.A.L. Leite^{26d}, R. Leitner¹³¹, D. Lellouch¹⁷⁵, B. Lemmer⁵⁷, K.J.C. Leney⁸¹, T. Lenz²³, B. Lenzi³², R. Leone⁷, S. Leone^{126a,126b}, C. Leonidopoulos⁴⁹, S. Leontsinis¹⁰, G. Lerner¹⁵¹, C. Leroy⁹⁷, A.A.J. Lesage¹³⁸, C.G. Lester³⁰, M. Levchenko¹²⁵, J. Levêque⁵, D. Levin⁹², L.J. Levinson¹⁷⁵, M. Levy¹⁹, D. Lewis⁷⁹, M. Leyton⁴⁴, B. Li^{36a,p}, C. Li^{36a}, H. Li¹⁵⁰, L. Li⁴⁸, L. Li^{36c}, Q. Li^{35a}, S. Li⁴⁸, X. Li⁸⁷, Y. Li¹⁴³, Z. Liang^{35a}, B. Liberti^{135a}, A. Liblong¹⁶¹, P. Lichard³², K. Lie¹⁶⁹, J. Liebal²³, W. Liebig¹⁵, A. Limosani¹⁵², S.C. Lin^{153,ab}, T.H. Lin⁸⁶, B.E. Lindquist¹⁵⁰, A.E. Lioni⁵², E. Lipeles¹²⁴, A. Lipniacka¹⁵, M. Lisovyi^{60b}, T.M. Liss¹⁶⁹, A. Lister¹⁷¹, A.M. Litke¹³⁹, B. Liu^{153,ac}, D. Liu¹⁵³, H. Liu⁹², H. Liu²⁷, J. Liu^{36b}, J.B. Liu^{36a}, K. Liu⁸⁸, L. Liu¹⁶⁹, M. Liu^{36a}, Y.L. Liu^{36a}, Y. Liu^{36a}, M. Livan^{123a,123b}, A. Lleres⁵⁸, J. Llorente Merino^{35a}, S.L. Lloyd⁷⁹, F. Lo Sterzo¹⁵³, E.M. Lobodzinska⁴⁵, P. Loch⁷, F.K. Loebinger⁸⁷, K.M. Loew²⁵, A. Loginov^{179,*}, T. Lohse¹⁷, K. Lohwasser⁴⁵, M. Lokajicek¹²⁹, B.A. Long²⁴, J.D. Long¹⁶⁹, R.E. Long⁷⁵, L. Longo^{76a,76b}, K.A. Looper¹¹³, J.A. Lopez^{34b}, D. Lopez Mateos⁵⁹, B. Lopez Paredes¹⁴¹, I. Lopez Paz¹³, A. Lopez Solis⁸³, J. Lorenz¹⁰², N. Lorenzo Martinez⁶⁴, M. Losada²¹, P.J. Lösel¹⁰², X. Lou^{35a}, A. Lounis¹¹⁹, J. Love⁶, P.A. Love⁷⁵, H. Lu^{62a}, N. Lu⁹², H.J. Lubatti¹⁴⁰, C. Luci^{134a,134b}, A. Lucotte⁵⁸, C. Luedtke⁵¹, F. Luehring⁶⁴, W. Lukas⁶⁵, L. Luminari^{134a}, O. Lundberg^{148a,148b}, B. Lund-Jensen¹⁴⁹, P.M. Luzzi⁸³, D. Lynn²⁷, R. Lysak¹²⁹, E. Lytken⁸⁴, V. Lyubushkin⁶⁸, H. Ma²⁷, L.L. Ma^{36b}, Y. Ma^{36b}, G. Maccarrone⁵⁰, A. Macchiolo¹⁰³, C.M. Macdonald¹⁴¹, B. Maček⁷⁸, J. Machado Miguens^{124,128b}, D. Madaffari⁸⁸, R. Madar³⁷, H.J. Maddocks¹⁶⁸, W.F. Mader⁴⁷, A. Madsen⁴⁵, J. Maeda⁷⁰, S. Maeland¹⁵, T. Maeno²⁷, A. Maevskiy¹⁰¹, E. Magradze⁵⁷, J. Mahlstedt¹⁰⁹, C. Maiani¹¹⁹, C. Maidantchik^{26a}, A.A. Maier¹⁰³, T. Maier¹⁰², A. Maio^{128a,128b,128d}, S. Majewski¹¹⁸, Y. Makida⁶⁹, N. Makovec¹¹⁹, B. Malaescu⁸³, Pa. Malecki⁴², V.P. Maleev¹²⁵, F. Malek⁵⁸, U. Mallik⁶⁶, D. Malon⁶, C. Malone¹⁴⁵, C. Malone³⁰, S. Maltezos¹⁰, S. Malyukov³², J. Mamuzic¹⁷⁰, G. Mancini⁵⁰, L. Mandelli^{94a}, I. Mandić⁷⁸, J. Maneira^{128a,128b}, L. Manhaes de Andrade Filho^{26b}, J. Manjarres Ramos^{163b}, A. Mann¹⁰², A. Manousos³², B. Mansoulie¹³⁸, J.D. Mansour^{35a}, R. Mantifel⁹⁰, M. Mantoani⁵⁷, S. Manzoni^{94a,94b}, L. Mapelli³², G. Marceca²⁹, L. March⁵², G. Marchiori⁸³, M. Marcisovsky¹²⁹, M. Marjanovic¹⁴, D.E. Marley⁹², F. Marroquim^{26a}, S.P. Marsden⁸⁷, Z. Marshall¹⁶, S. Marti-Garcia¹⁷⁰, B. Martin⁹³,

T.A. Martin¹⁷³, V.J. Martin⁴⁹, B. Martin dit Latour¹⁵, M. Martinez^{13,s}, V.I. Martinez Outschoorn¹⁶⁹, S. Martin-Haugh¹³³, V.S. Martoiu^{28b}, A.C. Martyniuk⁸¹, A. Marzin³², L. Masetti⁸⁶, T. Mashimo¹⁵⁷, R. Mashinistov⁹⁸, J. Masik⁸⁷, A.L. Maslennikov^{111,c}, I. Massa^{22a,22b}, L. Massa^{22a,22b}, P. Mastrandrea⁵, A. Mastroberardino^{40a,40b}, T. Masubuchi¹⁵⁷, P. Mättig¹⁷⁸, J. Mattmann⁸⁶, J. Maurer^{28b}, S.J. Maxfield⁷⁷, D.A. Maximov^{111,c}, R. Mazini¹⁵³, I. Maznas¹⁵⁶, S.M. Mazza^{94a,94b}, N.C. Mc Fadden¹⁰⁷, G. Mc Goldrick¹⁶¹, S.P. Mc Kee⁹², A. McCarn⁹², R.L. McCarthy¹⁵⁰, T.G. McCarthy¹⁰³, L.I. McClymont⁸¹, E.F. McDonald⁹¹, J.A. Mcfayden⁸¹, G. Mchedlidze⁵⁷, S.J. McMahon¹³³, R.A. McPherson^{172,m}, M. Medinnis⁴⁵, S. Meehan¹⁴⁰, S. Mehlhase¹⁰², A. Mehta⁷⁷, K. Meier^{60a}, C. Meineck¹⁰², B. Meirose⁴⁴, D. Melini^{170,ad}, B.R. Mellado Garcia^{147c}, M. Melo^{146a}, F. Meloni¹⁸, S.B. Menary⁸⁷, L. Meng⁷⁷, X.T. Meng⁹², A. Mengarelli^{22a,22b}, S. Menke¹⁰³, E. Meoni¹⁶⁵, S. Mergelmeyer¹⁷, P. Mermod⁵², L. Merola^{106a,106b}, C. Meroni^{94a}, F.S. Merritt³³, A. Messina^{134a,134b}, J. Metcalfe⁶, A.S. Mete¹⁶⁶, C. Meyer⁸⁶, C. Meyer¹²⁴, J.-P. Meyer¹³⁸, J. Meyer¹⁰⁹, H. Meyer Zu Theenhausen^{60a}, F. Miano¹⁵¹, R.P. Middleton¹³³, S. Miglioranza^{53a,53b}, L. Mijović⁴⁹, G. Mikenberg¹⁷⁵, M. Mikestikova¹²⁹, M. Mikuž⁷⁸, M. Milesi⁹¹, A. Milic²⁷, D.W. Miller³³, C. Mills⁴⁹, A. Milov¹⁷⁵, D.A. Milstead^{148a,148b}, A.A. Minaenko¹³², Y. Minami¹⁵⁷, I.A. Minashvili⁶⁸, A.I. Mincer¹¹², B. Mindur^{41a}, M. Mineev⁶⁸, Y. Minegishi¹⁵⁷, Y. Ming¹⁷⁶, L.M. Mir¹³, K.P. Mistry¹²⁴, T. Mitani¹⁷⁴, J. Mitrevski¹⁰², V.A. Mitsou¹⁷⁰, A. Miucci¹⁸, P.S. Miyagawa¹⁴¹, A. Mizukami⁶⁹, J.U. Mjörnmark⁸⁴, M. Mlynarikova¹³¹, T. Moa^{148a,148b}, K. Mochizuki⁹⁷, P. Mogg⁵¹, S. Mohapatra³⁸, S. Molander^{148a,148b}, R. Moles-Valls²³, R. Monden⁷¹, M.C. Mondragon⁹³, K. Mönig⁴⁵, J. Monk³⁹, E. Monnier⁸⁸, A. Montalbano¹⁵⁰, J. Montejo Berlingen³², F. Monticelli⁷⁴, S. Monzani^{94a,94b}, R.W. Moore³, N. Morange¹¹⁹, D. Moreno²¹, M. Moreno Llácer⁵⁷, P. Morettini^{53a}, S. Morgenstern³², D. Mori¹⁴⁴, T. Mori¹⁵⁷, M. Morii⁵⁹, M. Morinaga¹⁵⁷, V. Morisbak¹²¹, S. Moritz⁸⁶, A.K. Morley¹⁵², G. Mornacchi³², J.D. Morris⁷⁹, S.S. Mortensen³⁹, L. Morvaj¹⁵⁰, P. Moschovakos¹⁰, M. Mosidze^{54b}, H.J. Moss¹⁴¹, J. Moss^{145,ae}, K. Motohashi¹⁵⁹, R. Mount¹⁴⁵, E. Mountricha²⁷, E.J.W. Moyse⁸⁹, S. Muanza⁸⁸, R.D. Mudd¹⁹, F. Mueller¹⁰³, J. Mueller¹²⁷, R.S.P. Mueller¹⁰², T. Mueller³⁰, D. Muenstermann⁷⁵, P. Mullen⁵⁶, G.A. Mullier¹⁸, F.J. Munoz Sanchez⁸⁷, J.A. Murillo Quijada¹⁹, W.J. Murray^{173,133}, H. Musheghyan⁵⁷, M. Muškinja⁷⁸, A.G. Myagkov^{132,af}, M. Myska¹³⁰, B.P. Nachman¹⁴⁵, O. Nackenhorst⁵², K. Nagai¹²², R. Nagai^{69,z}, K. Nagano⁶⁹, Y. Nagasaka⁶¹, K. Nagata¹⁶⁴, M. Nagel⁵¹, E. Nagy⁸⁸, A.M. Nairz³², Y. Nakahama¹⁰⁵, K. Nakamura⁶⁹, T. Nakamura¹⁵⁷, I. Nakano¹¹⁴, R.F. Naranjo Garcia⁴⁵, R. Narayan¹¹, D.I. Narrias Villar^{60a}, I. Naryshkin¹²⁵, T. Naumann⁴⁵, G. Navarro²¹, R. Nayyar⁷, H.A. Neal⁹², P.Yu. Nechaeva⁹⁸, T.J. Neep⁸⁷, A. Negri^{123a,123b}, M. Negrini^{22a}, S. Nektarijevic¹⁰⁸, C. Nellist¹¹⁹, A. Nelson¹⁶⁶, S. Nemecek¹²⁹, P. Nemethy¹¹², A.A. Nepomuceno^{26a}, M. Nessi^{32,ag}, M.S. Neubauer¹⁶⁹, M. Neumann¹⁷⁸, R.M. Neves¹¹², P. Nevski²⁷, P.R. Newman¹⁹, D.H. Nguyen⁶, T. Nguyen Manh⁹⁷, R.B. Nickerson¹²², R. Nicolaidou¹³⁸, J. Nielsen¹³⁹, A. Nikiforov¹⁷, V. Nikolaenko^{132,af}, I. Nikolic-Audit⁸³, K. Nikolopoulos¹⁹, J.K. Nilsen¹²¹, P. Nilsson²⁷, Y. Ninomiya¹⁵⁷, A. Nisati^{134a}, R. Nisius¹⁰³, T. Nobe¹⁵⁷, M. Nomachi¹²⁰, I. Nomidis³¹, T. Nooney⁷⁹, S. Norberg¹¹⁵, M. Nordberg³², N. Norjoharuddeen¹²², O. Novgorodova⁴⁷, S. Nowak¹⁰³, M. Nozaki⁶⁹, L. Nozka¹¹⁷, K. Ntekas¹⁶⁶, E. Nurse⁸¹, F. Nuti⁹¹, F. O'grady⁷, D.C. O'Neil¹⁴⁴, A.A. O'Rourke⁴⁵, V. O'Shea⁵⁶, F.G. Oakham^{31,d}, H. Oberlack¹⁰³, T. Obermann²³, J. Ocariz⁸³, A. Ochi⁷⁰, I. Ochoa³⁸, J.P. Ochoa-Ricoux^{34a}, S. Oda⁷³, S. Odaka⁶⁹, H. Ogren⁶⁴, A. Oh⁸⁷, S.H. Oh⁴⁸, C.C. Ohm¹⁶, H. Ohman¹⁶⁸, H. Oide^{53a,53b}, H. Okawa¹⁶⁴, Y. Okumura¹⁵⁷, T. Okuyama⁶⁹, A. Olariu^{28b}, L.F. Oleiro Seabra^{128a}, S.A. Olivares Pino⁴⁹, D. Oliveira Damazio²⁷, A. Olszewski⁴², J. Olszowska⁴², A. Onofre^{128a,128e}, K. Onogi¹⁰⁵, P.U.E. Onyisi^{11,v}, M.J. Oreglia³³, Y. Oren¹⁵⁵, D. Orestano^{136a,136b}, N. Orlando^{62b}, R.S. Orr¹⁶¹, B. Osculati^{53a,53b,*}, R. Ospanov⁸⁷, G. Otero y Garzon²⁹, H. Otono⁷³, M. Ouchrif^{137d}, F. Ould-Saada¹²¹, A. Ouraou¹³⁸, K.P. Oussoren¹⁰⁹, Q. Ouyang^{35a}, M. Owen⁵⁶, R.E. Owen¹⁹, V.E. Ozcan^{20a}, N. Ozturk⁸, K. Pachal¹⁴⁴, A. Pacheco Pages¹³, L. Pacheco Rodriguez¹³⁸, C. Padilla Aranda¹³, S. Pagan Griso¹⁶, M. Paganini¹⁷⁹, F. Paige²⁷, P. Pais⁸⁹, K. Pajchel¹²¹, G. Palacino⁶⁴, S. Palazzo^{40a,40b}, S. Palestini³², M. Palka^{41b}, D. Pallin³⁷, E. St. Panagiotopoulou¹⁰, I. Panagoulas¹⁰, C.E. Pandini⁸³, J.G. Panduro Vazquez⁸⁰, P. Pani^{148a,148b}, S. Panitkin²⁷, D. Pantea^{28b}, L. Paolozzi⁵², Th.D. Papadopoulou¹⁰, K. Papageorgiou¹⁵⁶, A. Paramonov⁶, D. Paredes Hernandez¹⁷⁹, A.J. Parker⁷⁵, M.A. Parker³⁰, K.A. Parker¹⁴¹, F. Parodi^{53a,53b}, J.A. Parsons³⁸, U. Parzefall⁵¹, V.R. Pascuzzi¹⁶¹, E. Pasqualucci^{134a}, S. Passaggio^{53a}, Fr. Pastore⁸⁰, G. Pásztor^{31,ah}, S. Pataraia¹⁷⁸, J.R. Pater⁸⁷, T. Pauly³², J. Pearce¹⁷², B. Pearson¹¹⁵, L.E. Pedersen³⁹, M. Pedersen¹²¹, S. Pedraza Lopez¹⁷⁰, R. Pedro^{128a,128b}, S.V. Peleganchuk^{111,c}, O. Penc¹²⁹, C. Peng^{35a},

H. Peng^{36a}, J. Penwell⁶⁴, B.S. Peralva^{26b}, M.M. Perego¹³⁸, D.V. Perepelitsa²⁷, E. Perez Codina^{163a}, L. Perini^{94a,94b}, H. Pernegger³², S. Perrella^{106a,106b}, R. Peschke⁴⁵, V.D. Peshekhonov⁶⁸, K. Peters⁴⁵, R.F.Y. Peters⁸⁷, B.A. Petersen³², T.C. Petersen³⁹, E. Petit⁵⁸, A. Petridis¹, C. Petridou¹⁵⁶, P. Petroff¹¹⁹, E. Petrolo^{134a}, M. Petrov¹²², F. Petrucci^{136a,136b}, N.E. Pettersson⁸⁹, A. Peyaud¹³⁸, R. Pezoa^{34b}, P.W. Phillips¹³³, G. Piacquadio^{145,ai}, E. Pianori¹⁷³, A. Picazio⁸⁹, E. Piccaro⁷⁹, M. Piccinini^{22a,22b}, M.A. Pickering¹²², R. Piegai²⁹, J.E. Pilcher³³, A.D. Pilkington⁸⁷, A.W.J. Pin⁸⁷, M. Pinamonti^{167a,167c,aj}, J.L. Pinfold³, A. Pingel³⁹, S. Pires⁸³, H. Pirumov⁴⁵, M. Pitt¹⁷⁵, L. Plazak^{146a}, M.-A. Pleier²⁷, V. Pleskot⁸⁶, E. Plotnikova⁶⁸, D. Pluth⁶⁷, R. Poettgen^{148a,148b}, L. Poggioli¹¹⁹, D. Pohl²³, G. Polesello^{123a}, A. Poley⁴⁵, A. Policicchio^{40a,40b}, R. Polifka¹⁶¹, A. Polini^{22a}, C.S. Pollard⁵⁶, V. Polychronakos²⁷, K. Pommès³², L. Pontecorvo^{134a}, B.G. Pope⁹³, G.A. Popeneciu^{28c}, A. Poppleton³², S. Pospisil¹³⁰, K. Potamianos¹⁶, I.N. Potrap⁶⁸, C.J. Potter³⁰, C.T. Potter¹¹⁸, G. Poulard³², J. Poveda³², V. Pozdnyakov⁶⁸, M.E. Pozo Astigarraga³², P. Pralavorio⁸⁸, A. Pranko¹⁶, S. Prell⁶⁷, D. Price⁸⁷, L.E. Price⁶, M. Primavera^{76a}, S. Prince⁹⁰, K. Prokofiev^{62c}, F. Prokoshin^{34b}, S. Protopopescu²⁷, J. Proudfoot⁶, M. Przybycien^{41a}, D. Puddu^{136a,136b}, M. Purohit^{27,ak}, P. Puzo¹¹⁹, J. Qian⁹², G. Qin⁵⁶, Y. Qin⁸⁷, A. Quadt⁵⁷, W.B. Quayle^{167a,167b}, M. Queitsch-Maitland⁴⁵, D. Quilty⁵⁶, S. Raddum¹²¹, V. Radeka²⁷, V. Radescu¹²², S.K. Radhakrishnan¹⁵⁰, P. Radloff¹¹⁸, P. Rados⁹¹, F. Ragusa^{94a,94b}, G. Rahal¹⁸¹, J.A. Raine⁸⁷, S. Rajagopalan²⁷, M. Rammensee³², C. Rangel-Smith¹⁶⁸, M.G. Ratti^{94a,94b}, D.M. Rauch⁴⁵, F. Rauscher¹⁰², S. Rave⁸⁶, T. Ravenscroft⁵⁶, I. Ravinovich¹⁷⁵, M. Raymond³², A.L. Read¹²¹, N.P. Readioff⁷⁷, M. Reale^{76a,76b}, D.M. Rebuzzi^{123a,123b}, A. Redelbach¹⁷⁷, G. Redlinger²⁷, R. Reece¹³⁹, R.G. Reed^{147c}, K. Reeves⁴⁴, L. Rehnisch¹⁷, J. Reichert¹²⁴, A. Reiss⁸⁶, C. Rembser³², H. Ren^{35a}, M. Rescigno^{134a}, S. Resconi^{94a}, O.L. Rezanova^{111,c}, P. Reznicek¹³¹, R. Rezvani⁹⁷, R. Richter¹⁰³, S. Richter⁸¹, E. Richter-Was^{41b}, O. Ricken²³, M. Ridel⁸³, P. Rieck¹⁷, C.J. Riegel¹⁷⁸, J. Rieger⁵⁷, O. Rifki¹¹⁵, M. Rijssenbeek¹⁵⁰, A. Rimoldi^{123a,123b}, M. Rimoldi¹⁸, L. Rinaldi^{22a}, B. Ristić⁵², E. Ritsch³², I. Riu¹³, F. Rizatdinova¹¹⁶, E. Rizvi⁷⁹, C. Rizzi¹³, S.H. Robertson^{90,m}, A. Robichaud-Veronneau⁹⁰, D. Robinson³⁰, J.E.M. Robinson⁴⁵, A. Robson⁵⁶, C. Roda^{126a,126b}, Y. Rodina^{88,al}, A. Rodriguez Perez¹³, D. Rodriguez Rodriguez¹⁷⁰, S. Roe³², C.S. Rogan⁵⁹, O. Röhne¹²¹, J. Roloff⁵⁹, A. Romaniouk¹⁰⁰, M. Romano^{22a,22b}, S.M. Romano Saez³⁷, E. Romero Adam¹⁷⁰, N. Rompotis¹⁴⁰, M. Ronzani⁵¹, L. Roos⁸³, E. Ros¹⁷⁰, S. Rosati^{134a}, K. Rosbach⁵¹, P. Rose¹³⁹, N.-A. Rosien⁵⁷, V. Rossetti^{148a,148b}, E. Rossi^{106a,106b}, L.P. Rossi^{53a}, J.H.N. Rosten³⁰, R. Rosten¹⁴⁰, M. Rotaru^{28b}, I. Roth¹⁷⁵, J. Rothberg¹⁴⁰, D. Rousseau¹¹⁹, A. Rozanov⁸⁸, Y. Rozen¹⁵⁴, X. Ruan^{147c}, F. Rubbo¹⁴⁵, M.S. Rudolph¹⁶¹, F. Rühr⁵¹, A. Ruiz-Martinez³¹, Z. Rurikova⁵¹, N.A. Rusakovich⁶⁸, A. Ruschke¹⁰², H.L. Russell¹⁴⁰, J.P. Rutherford⁷, N. Ruthmann³², Y.F. Ryabov¹²⁵, M. Rybar¹⁶⁹, G. Rybkin¹¹⁹, S. Ryu⁶, A. Ryzhov¹³², G.F. Rzehorz⁵⁷, A.F. Saavedra¹⁵², G. Sabato¹⁰⁹, S. Sacerdoti²⁹, H.F.-W. Sadrozinski¹³⁹, R. Sadykov⁶⁸, F. Safai Tehrani^{134a}, P. Saha¹¹⁰, M. Sahinsoy^{60a}, M. Saimpert¹³⁸, T. Saito¹⁵⁷, H. Sakamoto¹⁵⁷, Y. Sakurai¹⁷⁴, G. Salamanna^{136a,136b}, A. Salamon^{135a,135b}, J.E. Salazar Loyola^{34b}, D. Salek¹⁰⁹, P.H. Sales De Bruin¹⁴⁰, D. Salihagic¹⁰³, A. Salnikov¹⁴⁵, J. Salt¹⁷⁰, D. Salvatore^{40a,40b}, F. Salvatore¹⁵¹, A. Salvucci^{62a,62b,62c}, A. Salzburger³², D. Sammel⁵¹, D. Sampsonidis¹⁵⁶, J. Sánchez¹⁷⁰, V. Sanchez Martinez¹⁷⁰, A. Sanchez Pineda^{106a,106b}, H. Sandaker¹²¹, R.L. Sandbach⁷⁹, M. Sandhoff¹⁷⁸, C. Sandoval²¹, D.P.C. Sankey¹³³, M. Sannino^{53a,53b}, A. Sansoni⁵⁰, C. Santoni³⁷, R. Santonico^{135a,135b}, H. Santos^{128a}, I. Santoyo Castillo¹⁵¹, K. Sapp¹²⁷, A. Saprnov⁶⁸, J.G. Saraiva^{128a,128d}, B. Sarrazin²³, O. Sasaki⁶⁹, K. Sato¹⁶⁴, E. Sauvan⁵, G. Savage⁸⁰, P. Savard^{161,d}, N. Savic¹⁰³, C. Sawyer¹³³, L. Sawyer^{82,r}, J. Saxon³³, C. Sbarra^{22a}, A. Sbrizzi^{22a,22b}, T. Scanlon⁸¹, D.A. Scannicchio¹⁶⁶, M. Scarcella¹⁵², V. Scarfone^{40a,40b}, J. Schaarschmidt¹⁷⁵, P. Schacht¹⁰³, B.M. Schachtner¹⁰², D. Schaefer³², L. Schaefer¹²⁴, R. Schaefer⁴⁵, J. Schaeffer⁸⁶, S. Schaepe²³, S. Schaetzel^{60b}, U. Schäfer⁸⁶, A.C. Schaffer¹¹⁹, D. Schaile¹⁰², R.D. Schamberger¹⁵⁰, V. Scharf^{60a}, V.A. Schegelsky¹²⁵, D. Scheirich¹³¹, M. Schernau¹⁶⁶, C. Schiavi^{53a,53b}, S. Schier¹³⁹, C. Schillo⁵¹, M. Schioppa^{40a,40b}, S. Schlenker³², K.R. Schmidt-Sommerfeld¹⁰³, K. Schmieden³², C. Schmitt⁸⁶, S. Schmitt⁴⁵, S. Schmitz⁸⁶, B. Schneider^{163a}, U. Schnoor⁵¹, L. Schoeffel¹³⁸, A. Schoening^{60b}, B.D. Schoenrock⁹³, E. Schopf²³, M. Schott⁸⁶, J.F.P. Schouwenberg¹⁰⁸, J. Schovancova⁸, S. Schramm⁵², M. Schreyer¹⁷⁷, N. Schuh⁸⁶, A. Schulte⁸⁶, M.J. Schultens²³, H.-C. Schultz-Coulon^{60a}, H. Schulz¹⁷, M. Schumacher⁵¹, B.A. Schumm¹³⁹, Ph. Schune¹³⁸, A. Schwartzman¹⁴⁵, T.A. Schwarz⁹², H. Schweiger⁸⁷, Ph. Schwemling¹³⁸, R. Schwienhorst⁹³, J. Schwindling¹³⁸, T. Schwindt²³, G. Sciolla²⁵, F. Scuri^{126a,126b}, F. Scutti⁹¹, J. Searcy⁹², P. Seema²³, S.C. Seidel¹⁰⁷, A. Seiden¹³⁹, F. Seifert¹³⁰, J.M. Seixas^{26a},

G. Sekhniaidze^{106a}, K. Sekhon⁹², S.J. Sekula⁴³, D.M. Seliverstov^{125,*}, N. Semprini-Cesari^{22a,22b},
 C. Serfon¹²¹, L. Serin¹¹⁹, L. Serkin^{167a,167b}, M. Sessa^{136a,136b}, R. Seuster¹⁷², H. Severini¹¹⁵, T. Sfiligoi⁷⁸,
 F. Sforza³², A. Sfyrta⁵², E. Shabalina⁵⁷, N.W. Shaikh^{148a,148b}, L.Y. Shan^{35a}, R. Shang¹⁶⁹, J.T. Shank²⁴,
 M. Shapiro¹⁶, P.B. Shatalov⁹⁹, K. Shaw^{167a,167b}, S.M. Shaw⁸⁷, A. Shcherbakova^{148a,148b}, C.Y. Shehu¹⁵¹,
 P. Sherwood⁸¹, L. Shi^{153,am}, S. Shimizu⁷⁰, C.O. Shimmin¹⁶⁶, M. Shimojima¹⁰⁴, S. Shirabe⁷³,
 M. Shiyakova^{68,an}, A. Shmeleva⁹⁸, D. Shoaleh Saadi⁹⁷, M.J. Shochet³³, S. Shojaii^{94a}, D.R. Shope¹¹⁵,
 S. Shrestha¹¹³, E. Shulga¹⁰⁰, M.A. Shupe⁷, P. Sicho¹²⁹, A.M. Sickles¹⁶⁹, P.E. Sidebo¹⁴⁹,
 E. Sideras Haddad^{147c}, O. Sidiropoulou¹⁷⁷, D. Sidorov¹¹⁶, A. Sidoti^{22a,22b}, F. Siegert⁴⁷, Dj. Sijacki¹⁴,
 J. Silva^{128a,128d}, S.B. Silverstein^{148a}, V. Simak¹³⁰, Lj. Simic¹⁴, S. Simion¹¹⁹, E. Simioni⁸⁶, B. Simmons⁸¹,
 D. Simon³⁷, M. Simon⁸⁶, P. Sinervo¹⁶¹, N.B. Sinev¹¹⁸, M. Sioli^{22a,22b}, G. Siragusa¹⁷⁷, S.Yu. Sivoklokov¹⁰¹,
 J. Sjölin^{148a,148b}, M.B. Skinner⁷⁵, H.P. Skottowe⁵⁹, P. Skubic¹¹⁵, M. Slater¹⁹, T. Slavicek¹³⁰,
 M. Slawinska¹⁰⁹, K. Sliwa¹⁶⁵, R. Slovak¹³¹, V. Smakhtin¹⁷⁵, B.H. Smart⁵, L. Smestad¹⁵, J. Smiesko^{146a},
 S.Yu. Smirnov¹⁰⁰, Y. Smirnov¹⁰⁰, L.N. Smirnova^{101,ao}, O. Smirnova⁸⁴, J.W. Smith⁵⁷, M.N.K. Smith³⁸,
 R.W. Smith³⁸, M. Smizanska⁷⁵, K. Smolek¹³⁰, A.A. Snesev⁹⁸, I.M. Snyder¹¹⁸, S. Snyder²⁷,
 R. Sobie^{172,m}, F. Socher⁴⁷, A. Soffer¹⁵⁵, D.A. Soh¹⁵³, G. Sokhrannyi⁷⁸, C.A. Solans Sanchez³²,
 M. Solar¹³⁰, E.Yu. Soldatov¹⁰⁰, U. Soldevila¹⁷⁰, A.A. Solodkov¹³², A. Soloshenko⁶⁸, O.V. Solovyanov¹³²,
 V. Solovyev¹²⁵, P. Sommer⁵¹, H. Son¹⁶⁵, H.Y. Song^{36a,ap}, A. Sood¹⁶, A. Sopczak¹³⁰, V. Sopko¹³⁰,
 V. Sorin¹³, D. Sosa^{60b}, C.L. Sotiropoulou^{126a,126b}, R. Soualah^{167a,167c}, A.M. Soukharev^{111,c}, D. South⁴⁵,
 B.C. Sowden⁸⁰, S. Spagnolo^{76a,76b}, M. Spalla^{126a,126b}, M. Spangenberg¹⁷³, F. Spanò⁸⁰, D. Sperlich¹⁷,
 F. Spettel¹⁰³, R. Spighi^{22a}, G. Spigo³², L.A. Spiller⁹¹, M. Spousta¹³¹, R.D. St. Denis^{56,*}, A. Stabile^{94a},
 R. Stamen^{60a}, S. Stamm¹⁷, E. Stanecka⁴², R.W. Stanek⁶, C. Stanescu^{136a}, M. Stanescu-Bellu⁴⁵,
 M.M. Stanitzki⁴⁵, S. Stapnes¹²¹, E.A. Starchenko¹³², G.H. Stark³³, J. Stark⁵⁸, P. Staroba¹²⁹,
 P. Starovoitov^{60a}, S. Stärz³², R. Staszewski⁴², P. Steinberg²⁷, B. Stelzer¹⁴⁴, H.J. Stelzer³²,
 O. Stelzer-Chilton^{163a}, H. Stenzel⁵⁵, G.A. Stewart⁵⁶, J.A. Stillings²³, M.C. Stockton⁹⁰, M. Stoebe⁹⁰,
 G. Stoicea^{28b}, P. Stolte⁵⁷, S. Stonjek¹⁰³, A.R. Stradling⁸, A. Straessner⁴⁷, M.E. Stramaglia¹⁸,
 J. Strandberg¹⁴⁹, S. Strandberg^{148a,148b}, A. Strandlie¹²¹, M. Strauss¹¹⁵, P. Strizenec^{146b}, R. Ströhmer¹⁷⁷,
 D.M. Strom¹¹⁸, R. Stroynowski⁴³, A. Strubig¹⁰⁸, S.A. Stucci²⁷, B. Stugu¹⁵, N.A. Styles⁴⁵, D. Su¹⁴⁵,
 J. Su¹²⁷, S. Suchek^{60a}, Y. Sugaya¹²⁰, M. Suk¹³⁰, V.V. Sulin⁹⁸, S. Sultansoy^{4c}, T. Sumida⁷¹, S. Sun⁵⁹,
 X. Sun^{35a}, J.E. Sundermann⁵¹, K. Suruliz¹⁵¹, C.J.E. Suster¹⁵², M.R. Sutton¹⁵¹, S. Suzuki⁶⁹, M. Svatos¹²⁹,
 M. Swiatlowski³³, S.P. Swift², I. Sykora^{146a}, T. Sykora¹³¹, D. Ta⁵¹, C. Taccini^{136a,136b}, K. Tackmann⁴⁵,
 J. Taenzer¹⁵⁵, A. Taffard¹⁶⁶, R. Tafirot^{163a}, N. Taiblum¹⁵⁵, H. Takai²⁷, R. Takashima⁷², T. Takeshita¹⁴²,
 Y. Takubo⁶⁹, M. Talby⁸⁸, A.A. Talyshv^{111,c}, K.G. Tan⁹¹, J. Tanaka¹⁵⁷, M. Tanaka¹⁵⁹, R. Tanaka¹¹⁹,
 S. Tanaka⁶⁹, R. Tanioka⁷⁰, B.B. Tannenwald¹¹³, S. Tapia Araya^{34b}, S. Tapprogge⁸⁶, S. Tarem¹⁵⁴,
 G.F. Tartarelli^{94a}, P. Tas¹³¹, M. Tasevsky¹²⁹, T. Tashiro⁷¹, E. Tassi^{40a,40b}, A. Tavares Delgado^{128a,128b},
 Y. Tayalati^{137e}, A.C. Taylor¹⁰⁷, G.N. Taylor⁹¹, P.T.E. Taylor⁹¹, W. Taylor^{163b}, F.A. Teischinger³²,
 P. Teixeira-Dias⁸⁰, K.K. Temming⁵¹, D. Temple¹⁴⁴, H. Ten Kate³², P.K. Teng¹⁵³, J.J. Teoh¹²⁰, F. Tepel¹⁷⁸,
 S. Terada⁶⁹, K. Terashi¹⁵⁷, J. Terron⁸⁵, S. Terzo¹³, M. Testa⁵⁰, R.J. Teuscher^{161,m}, T. Theveneaux-Pelzer⁸⁸,
 J.P. Thomas¹⁹, J. Thomas-Wilsker⁸⁰, P.D. Thompson¹⁹, A.S. Thompson⁵⁶, L.A. Thomsen¹⁷⁹,
 E. Thomson¹²⁴, M.J. Tibbetts¹⁶, R.E. Ticse Torres⁸⁸, V.O. Tikhomirov^{98,aq}, Yu.A. Tikhonov^{111,c},
 S. Timoshenko¹⁰⁰, P. Tipton¹⁷⁹, S. Tisserant⁸⁸, K. Todome¹⁵⁹, T. Todorov^{5,*}, S. Todorova-Nova¹³¹,
 J. Tojo⁷³, S. Tokár^{146a}, K. Tokushuku⁶⁹, E. Tolley⁵⁹, L. Tomlinson⁸⁷, M. Tomoto¹⁰⁵, L. Tompkins^{145,ar},
 K. Toms¹⁰⁷, B. Tong⁵⁹, P. Tornambe⁵¹, E. Torrence¹¹⁸, H. Torres¹⁴⁴, E. Torró Pastor¹⁴⁰, J. Toth^{88,as},
 F. Touchard⁸⁸, D.R. Tovey¹⁴¹, T. Trefzger¹⁷⁷, A. Tricoli²⁷, I.M. Trigger^{163a}, S. Trincas-Duvold⁸³,
 M.F. Tripiana¹³, W. Trischuk¹⁶¹, B. Trocmé⁵⁸, A. Trofymov⁴⁵, C. Troncon^{94a}, M. Trotter-McDonald¹⁶,
 M. Trovatelli¹⁷², L. Truong^{167a,167c}, M. Trzebinski⁴², A. Trzupek⁴², J.C.-L. Tseng¹²², P.V. Tsiareshka⁹⁵,
 G. Tsipolitis¹⁰, N. Tsirintanis⁹, S. Tsiskaridze¹³, V. Tsiskaridze⁵¹, E.G. Tskhadadze^{54a}, K.M. Tsui^{62a},
 I.I. Tsukerman⁹⁹, V. Tsulaia¹⁶, S. Tsuno⁶⁹, D. Tsybychev¹⁵⁰, Y. Tu^{62b}, A. Tudorache^{28b}, V. Tudorache^{28b},
 T.T. Tulbure^{28a}, A.N. Tuna⁵⁹, S.A. Tupputi^{22a,22b}, S. Turchikhin⁶⁸, D. Turgeman¹⁷⁵, I. Turk Cakir^{4b,at},
 R. Turra^{94a,94b}, P.M. Tuts³⁸, G. Ucchielli^{22a,22b}, I. Ueda¹⁵⁷, M. Ughetto^{148a,148b}, F. Ukegawa¹⁶⁴,
 G. Unal³², A. Undrus²⁷, G. Unel¹⁶⁶, F.C. Ungaro⁹¹, Y. Unno⁶⁹, C. Unverdorben¹⁰², J. Urban^{146b},
 P. Urquijo⁹¹, P. Urrejola⁸⁶, G. Usai⁸, J. Usui⁶⁹, L. Vacavant⁸⁸, V. Vacek¹³⁰, B. Vachon⁹⁰, C. Valderanis¹⁰²,
 E. Valdes Santurio^{148a,148b}, N. Valencic¹⁰⁹, S. Valentini^{22a,22b}, A. Valero¹⁷⁰, L. Valery¹³, S. Valkar¹³¹,

J.A. Valls Ferrer¹⁷⁰, W. Van Den Wollenberg¹⁰⁹, P.C. Van Der Deijl¹⁰⁹, H. van der Graaf¹⁰⁹, N. van Eldik¹⁵⁴, P. van Gemmeren⁶, J. Van Nieuwkoop¹⁴⁴, I. van Vulpen¹⁰⁹, M.C. van Woerden¹⁰⁹, M. Vanadia^{134a,134b}, W. Vandelli³², R. Vanguri¹²⁴, A. Vaniachine¹⁶⁰, P. Vankov¹⁰⁹, G. Vardanyan¹⁸⁰, R. Vari^{134a}, E.W. Varnes⁷, T. Varol⁴³, D. Varouchas⁸³, A. Vartapetian⁸, K.E. Varvell¹⁵², J.G. Vasquez¹⁷⁹, G.A. Vasquez^{34b}, F. Vazeille³⁷, T. Vazquez Schroeder⁹⁰, J. Veatch⁵⁷, V. Veeraraghavan⁷, L.M. Veloce¹⁶¹, F. Veloso^{128a,128c}, S. Veneziano^{134a}, A. Ventura^{76a,76b}, M. Venturi¹⁷², N. Venturi¹⁶¹, A. Venturini²⁵, V. Vercesi^{123a}, M. Verducci^{134a,134b}, W. Verkerke¹⁰⁹, J.C. Vermeulen¹⁰⁹, A. Vest^{47,au}, M.C. Vetterli^{144,d}, O. Viazlo⁸⁴, I. Vichou^{169,*}, T. Vickey¹⁴¹, O.E. Vickey Boeriu¹⁴¹, G.H.A. Viehhauser¹²², S. Viel¹⁶, L. Vigani¹²², M. Villa^{22a,22b}, M. Villaplana Perez^{94a,94b}, E. Vilucchi⁵⁰, M.G. Vinciter³¹, V.B. Vinogradov⁶⁸, C. Vittori^{22a,22b}, I. Vivarelli¹⁵¹, S. Vlachos¹⁰, M. Vlasak¹³⁰, M. Vogel¹⁷⁸, P. Vokac¹³⁰, G. Volpi^{126a,126b}, M. Volpi⁹¹, H. von der Schmitt¹⁰³, E. von Toerne²³, V. Vorobel¹³¹, K. Vorobev¹⁰⁰, M. Vos¹⁷⁰, R. Voss³², J.H. Vossebeld⁷⁷, N. Vranjes¹⁴, M. Vranjes Milosavljevic¹⁴, V. Vrba¹²⁹, M. Vreeswijk¹⁰⁹, R. Vuillermet³², I. Vukotic³³, P. Wagner²³, W. Wagner¹⁷⁸, H. Wahlberg⁷⁴, S. Wahrmund⁴⁷, J. Wakabayashi¹⁰⁵, J. Walder⁷⁵, R. Walker¹⁰², W. Walkowiak¹⁴³, V. Wallangen^{148a,148b}, C. Wang^{35b}, C. Wang^{36b,av}, F. Wang¹⁷⁶, H. Wang¹⁶, H. Wang⁴³, J. Wang⁴⁵, J. Wang¹⁵², K. Wang⁹⁰, R. Wang⁶, S.M. Wang¹⁵³, T. Wang³⁸, W. Wang^{36a}, C. Wanotayaroj¹¹⁸, A. Warburton⁹⁰, C.P. Ward³⁰, D.R. Wardrope⁸¹, A. Washbrook⁴⁹, P.M. Watkins¹⁹, A.T. Watson¹⁹, M.F. Watson¹⁹, G. Watts¹⁴⁰, S. Watts⁸⁷, B.M. Waugh⁸¹, S. Webb⁸⁶, M.S. Weber¹⁸, S.W. Weber¹⁷⁷, S.A. Weber³¹, J.S. Webster⁶, A.R. Weidberg¹²², B. Weinert⁶⁴, J. Weingarten⁵⁷, C. Weiser⁵¹, H. Weits¹⁰⁹, P.S. Wells³², T. Wenaus²⁷, T. Wengler³², S. Wenig³², N. Wermes²³, M.D. Werner⁶⁷, P. Werner³², M. Wessels^{60a}, J. Wetter¹⁶⁵, K. Whalen¹¹⁸, N.L. Whallon¹⁴⁰, A.M. Wharton⁷⁵, A. White⁸, M.J. White¹, R. White^{34b}, D. Whiteson¹⁶⁶, F.J. Wickens¹³³, W. Wiedenmann¹⁷⁶, M. Wielers¹³³, C. Wiglesworth³⁹, L.A.M. Wiik-Fuchs²³, A. Wildauer¹⁰³, F. Wilk⁸⁷, H.G. Wilkens³², H.H. Williams¹²⁴, S. Williams¹⁰⁹, C. Willis⁹³, S. Willocq⁸⁹, J.A. Wilson¹⁹, I. Wingerter-Seez⁵, F. Winklmeier¹¹⁸, O.J. Winston¹⁵¹, B.T. Winter²³, M. Wittgen¹⁴⁵, T.M.H. Wolf¹⁰⁹, R. Wolff⁸⁸, M.W. Wolter⁴², H. Wolters^{128a,128c}, S.D. Worm¹³³, B.K. Wosiek⁴², J. Wotschack³², M.J. Woudstra⁸⁷, K.W. Wozniak⁴², M. Wu⁵⁸, M. Wu³³, S.L. Wu¹⁷⁶, X. Wu⁵², Y. Wu⁹², T.R. Wyatt⁸⁷, B.M. Wynne⁴⁹, S. Xella³⁹, Z. Xi⁹², D. Xu^{35a}, L. Xu²⁷, B. Yabsley¹⁵², S. Yacooob^{147a}, D. Yamaguchi¹⁵⁹, Y. Yamaguchi¹²⁰, A. Yamamoto⁶⁹, S. Yamamoto¹⁵⁷, T. Yamanaka¹⁵⁷, K. Yamauchi¹⁰⁵, Y. Yamazaki⁷⁰, Z. Yan²⁴, H. Yang^{36c}, H. Yang¹⁷⁶, Y. Yang¹⁵³, Z. Yang¹⁵, W.-M. Yao¹⁶, Y.C. Yap⁸³, Y. Yasu⁶⁹, E. Yatsenko⁵, K.H. Yau Wong²³, J. Ye⁴³, S. Ye²⁷, I. Yeletsikh⁶⁸, E. Yildirim⁸⁶, K. Yorita¹⁷⁴, R. Yoshida⁶, K. Yoshihara¹²⁴, C. Young¹⁴⁵, C.J.S. Young³², S. Youssef²⁴, D.R. Yu¹⁶, J. Yu⁸, J.M. Yu⁹², J. Yu⁶⁷, L. Yuan⁷⁰, S.P.Y. Yuen²³, I. Yusuff^{30,aw}, B. Zabinski⁴², G. Zacharis¹⁰, R. Zaidan⁶⁶, A.M. Zaitsev^{132,af}, N. Zakharchuk⁴⁵, J. Zalieckas¹⁵, A. Zaman¹⁵⁰, S. Zambito⁵⁹, L. Zanello^{134a,134b}, D. Zanzi⁹¹, C. Zeitnitz¹⁷⁸, M. Zeman¹³⁰, A. Zemla^{41a}, J.C. Zeng¹⁶⁹, Q. Zeng¹⁴⁵, O. Zenin¹³², T. Ženiš^{146a}, D. Zerwas¹¹⁹, D. Zhang⁹², F. Zhang¹⁷⁶, G. Zhang^{36a,ap}, H. Zhang^{35b}, J. Zhang⁶, L. Zhang⁵¹, L. Zhang^{36a}, M. Zhang¹⁶⁹, R. Zhang²³, R. Zhang^{36a,av}, X. Zhang^{36b}, Z. Zhang¹¹⁹, X. Zhao⁴³, Y. Zhao^{36b,ax}, Z. Zhao^{36a}, A. Zhemchugov⁶⁸, J. Zhong¹²², B. Zhou⁹², C. Zhou¹⁷⁶, L. Zhou³⁸, L. Zhou⁴³, M. Zhou¹⁵⁰, N. Zhou^{35c}, C.G. Zhu^{36b}, H. Zhu^{35a}, J. Zhu⁹², Y. Zhu^{36a}, X. Zhuang^{35a}, K. Zhukov⁹⁸, A. Zibell¹⁷⁷, D. Zieminska⁶⁴, N.I. Zimine⁶⁸, C. Zimmermann⁸⁶, S. Zimmermann⁵¹, Z. Zinonos⁵⁷, M. Zinser⁸⁶, M. Ziolkowski¹⁴³, L. Živković¹⁴, G. Zobernig¹⁷⁶, A. Zoccoli^{22a,22b}, M. zur Nedden¹⁷, L. Zwalinski³²

¹ Department of Physics, University of Adelaide, Adelaide, Australia² Physics Department, SUNY Albany, Albany NY, United States³ Department of Physics, University of Alberta, Edmonton AB, Canada⁴ (a) Department of Physics, Ankara University, Ankara; (b) Istanbul Aydin University, Istanbul; (c) Division of Physics, TOBB University of Economics and Technology, Ankara, Turkey⁵ LAPP, CNRS/IN2P3 and Université Savoie Mont Blanc, Annecy-le-Vieux, France⁶ High Energy Physics Division, Argonne National Laboratory, Argonne IL, United States⁷ Department of Physics, University of Arizona, Tucson AZ, United States⁸ Department of Physics, The University of Texas at Arlington, Arlington TX, United States⁹ Physics Department, National and Kapodistrian University of Athens, Athens, Greece¹⁰ Physics Department, National Technical University of Athens, Zografou, Greece¹¹ Department of Physics, The University of Texas at Austin, Austin TX, United States¹² Institute of Physics, Azerbaijan Academy of Sciences, Baku, Azerbaijan¹³ Institut de Física d'Altes Energies (IFAE), The Barcelona Institute of Science and Technology, Barcelona, Spain¹⁴ Institute of Physics, University of Belgrade, Belgrade, Serbia¹⁵ Department for Physics and Technology, University of Bergen, Bergen, Norway¹⁶ Physics Division, Lawrence Berkeley National Laboratory and University of California, Berkeley CA, United States

- ¹⁷ Department of Physics, Humboldt University, Berlin, Germany
- ¹⁸ Albert Einstein Center for Fundamental Physics and Laboratory for High Energy Physics, University of Bern, Bern, Switzerland
- ¹⁹ School of Physics and Astronomy, University of Birmingham, Birmingham, United Kingdom
- ²⁰ (a) Department of Physics, Bogazici University, Istanbul; (b) Department of Physics Engineering, Gaziantep University, Gaziantep; (d) Istanbul Bilgi University, Faculty of Engineering and Natural Sciences, Istanbul, Turkey; (e) Bahcesehir University, Faculty of Engineering and Natural Sciences, Istanbul, Turkey
- ²¹ Centro de Investigaciones, Universidad Antonio Narino, Bogota, Colombia
- ²² (a) INFN Sezione di Bologna; (b) Dipartimento di Fisica e Astronomia, Università di Bologna, Bologna, Italy
- ²³ Physikalisches Institut, University of Bonn, Bonn, Germany
- ²⁴ Department of Physics, Boston University, Boston MA, United States
- ²⁵ Department of Physics, Brandeis University, Waltham MA, United States
- ²⁶ (a) Universidade Federal do Rio De Janeiro COPPE/EE/IF, Rio de Janeiro; (b) Electrical Circuits Department, Federal University of Juiz de Fora (UFJF), Juiz de Fora; (c) Federal University of Sao Joao del Rei (UFSJ), Sao Joao del Rei; (d) Instituto de Fisica, Universidade de Sao Paulo, Sao Paulo, Brazil
- ²⁷ Physics Department, Brookhaven National Laboratory, Upton NY, United States
- ²⁸ (a) Transilvania University of Brasov, Brasov, Romania; (b) Horia Hulubei National Institute of Physics and Nuclear Engineering, Bucharest; (c) National Institute for Research and Development of Isotopic and Molecular Technologies, Physics Department, Cluj Napoca; (d) University Politehnica Bucharest, Bucharest; (e) West University in Timisoara, Timisoara, Romania
- ²⁹ Departamento de Fisica, Universidad de Buenos Aires, Buenos Aires, Argentina
- ³⁰ Cavendish Laboratory, University of Cambridge, Cambridge, United Kingdom
- ³¹ Department of Physics, Carleton University, Ottawa ON, Canada
- ³² CERN, Geneva, Switzerland
- ³³ Enrico Fermi Institute, University of Chicago, Chicago IL, United States
- ³⁴ (a) Departamento de Fisica, Pontificia Universidad Católica de Chile, Santiago; (b) Departamento de Fisica, Universidad Técnica Federico Santa María, Valparaíso, Chile
- ³⁵ (a) Institute of High Energy Physics, Chinese Academy of Sciences, Beijing; (b) Department of Physics, Nanjing University, Jiangsu; (c) Physics Department, Tsinghua University, Beijing 100084, China
- ³⁶ (a) Department of Modern Physics, University of Science and Technology of China, Anhui; (b) School of Physics, Shandong University, Shandong; (c) Department of Physics and Astronomy, Shanghai Key Laboratory for Particle Physics and Cosmology, Shanghai Jiao Tong University, Shanghai, China ³⁷
- ³⁷ Laboratoire de Physique Corpusculaire, Université Clermont Auvergne, Université Blaise Pascal, CNRS/IN2P3, Clermont-Ferrand, France
- ³⁸ Nevis Laboratory, Columbia University, Irvington NY, United States
- ³⁹ Niels Bohr Institute, University of Copenhagen, Copenhagen, Denmark
- ⁴⁰ (a) INFN Gruppo Collegato di Cosenza, Laboratori Nazionali di Frascati; (b) Dipartimento di Fisica, Università della Calabria, Rende, Italy
- ⁴¹ (a) AGH University of Science and Technology, Faculty of Physics and Applied Computer Science, Krakow; (b) Marian Smoluchowski Institute of Physics, Jagiellonian University, Krakow, Poland
- ⁴² Institute of Nuclear Physics Polish Academy of Sciences, Krakow, Poland
- ⁴³ Physics Department, Southern Methodist University, Dallas TX, United States
- ⁴⁴ Physics Department, University of Texas at Dallas, Richardson TX, United States
- ⁴⁵ DESY, Hamburg and Zeuthen, Germany
- ⁴⁶ Lehrstuhl für Experimentelle Physik IV, Technische Universität Dortmund, Dortmund, Germany
- ⁴⁷ Institut für Kern- und Teilchenphysik, Technische Universität Dresden, Dresden, Germany
- ⁴⁸ Department of Physics, Duke University, Durham NC, United States
- ⁴⁹ SUPA – School of Physics and Astronomy, University of Edinburgh, Edinburgh, United Kingdom
- ⁵⁰ INFN Laboratori Nazionali di Frascati, Frascati, Italy
- ⁵¹ Fakultät für Mathematik und Physik, Albert-Ludwigs-Universität, Freiburg, Germany
- ⁵² Departement de Physique Nucleaire et Corpusculaire, Université de Genève, Geneva, Switzerland
- ⁵³ (a) INFN Sezione di Genova; (b) Dipartimento di Fisica, Università di Genova, Genova, Italy
- ⁵⁴ (a) E. Andronikashvili Institute of Physics, Iv. Javakishvili Tbilisi State University, Tbilisi; (b) High Energy Physics Institute, Tbilisi State University, Tbilisi, Georgia
- ⁵⁵ II Physikalisches Institut, Justus-Liebig-Universität Giessen, Giessen, Germany
- ⁵⁶ SUPA – School of Physics and Astronomy, University of Glasgow, Glasgow, United Kingdom
- ⁵⁷ II Physikalisches Institut, Georg-August-Universität, Göttingen, Germany
- ⁵⁸ Laboratoire de Physique Subatomique et de Cosmologie, Université Grenoble-Alpes, CNRS/IN2P3, Grenoble, France
- ⁵⁹ Laboratory for Particle Physics and Cosmology, Harvard University, Cambridge MA, United States
- ⁶⁰ (a) Kirchhoff-Institut für Physik, Ruprecht-Karls-Universität Heidelberg, Heidelberg; (b) Physikalisches Institut, Ruprecht-Karls-Universität Heidelberg, Heidelberg; (c) ZITI Institut für technische Informatik, Ruprecht-Karls-Universität Heidelberg, Mannheim, Germany
- ⁶¹ Faculty of Applied Information Science, Hiroshima Institute of Technology, Hiroshima, Japan
- ⁶² (a) Department of Physics, The Chinese University of Hong Kong, Shatin, N.T., Hong Kong; (b) Department of Physics, The University of Hong Kong, Hong Kong; (c) Department of Physics and Institute for Advanced Study, The Hong Kong University of Science and Technology, Clear Water Bay, Kowloon, Hong Kong, China
- ⁶³ Department of Physics, National Tsing Hua University, Taiwan, Taiwan
- ⁶⁴ Department of Physics, Indiana University, Bloomington IN, United States
- ⁶⁵ Institut für Astro- und Teilchenphysik, Leopold-Franzens-Universität, Innsbruck, Austria
- ⁶⁶ University of Iowa, Iowa City IA, United States
- ⁶⁷ Department of Physics and Astronomy, Iowa State University, Ames IA, United States
- ⁶⁸ Joint Institute for Nuclear Research, JINR Dubna, Dubna, Russia
- ⁶⁹ KEK, High Energy Accelerator Research Organization, Tsukuba, Japan
- ⁷⁰ Graduate School of Science, Kobe University, Kobe, Japan
- ⁷¹ Faculty of Science, Kyoto University, Kyoto, Japan
- ⁷² Kyoto University of Education, Kyoto, Japan
- ⁷³ Department of Physics, Kyushu University, Fukuoka, Japan
- ⁷⁴ Instituto de Fisica La Plata, Universidad Nacional de La Plata and CONICET, La Plata, Argentina
- ⁷⁵ Physics Department, Lancaster University, Lancaster, United Kingdom
- ⁷⁶ (a) INFN Sezione di Lecce; (b) Dipartimento di Matematica e Fisica, Università del Salento, Lecce, Italy
- ⁷⁷ Oliver Lodge Laboratory, University of Liverpool, Liverpool, United Kingdom
- ⁷⁸ Department of Experimental Particle Physics, Jožef Stefan Institute and Department of Physics, University of Ljubljana, Ljubljana, Slovenia
- ⁷⁹ School of Physics and Astronomy, Queen Mary University of London, London, United Kingdom
- ⁸⁰ Department of Physics, Royal Holloway University of London, Surrey, United Kingdom
- ⁸¹ Department of Physics and Astronomy, University College London, London, United Kingdom
- ⁸² Louisiana Tech University, Ruston LA, United States
- ⁸³ Laboratoire de Physique Nucléaire et de Hautes Energies, UPMC and Université Paris-Diderot and CNRS/IN2P3, Paris, France
- ⁸⁴ Fysiska institutionen, Lunds universitet, Lund, Sweden
- ⁸⁵ Departamento de Fisica Teorica C-15, Universidad Autonoma de Madrid, Madrid, Spain
- ⁸⁶ Institut für Physik, Universität Mainz, Mainz, Germany

- ⁸⁷ School of Physics and Astronomy, University of Manchester, Manchester, United Kingdom
- ⁸⁸ CPPM, Aix-Marseille Université et CNRS/IN2P3, Marseille, France
- ⁸⁹ Department of Physics, University of Massachusetts, Amherst MA, United States
- ⁹⁰ Department of Physics, McGill University, Montreal QC, Canada
- ⁹¹ School of Physics, University of Melbourne, Victoria, Australia
- ⁹² Department of Physics, The University of Michigan, Ann Arbor MI, United States
- ⁹³ Department of Physics and Astronomy, Michigan State University, East Lansing MI, United States
- ⁹⁴ ^(a) INFN Sezione di Milano; ^(b) Dipartimento di Fisica, Università di Milano, Milano, Italy
- ⁹⁵ B.I. Stepanov Institute of Physics, National Academy of Sciences of Belarus, Minsk, Belarus
- ⁹⁶ Research Institute for Nuclear Problems of Byelorussian State University, Minsk, Belarus
- ⁹⁷ Group of Particle Physics, University of Montreal, Montreal QC, Canada
- ⁹⁸ P.N. Lebedev Physical Institute of the Russian Academy of Sciences, Moscow, Russia
- ⁹⁹ Institute for Theoretical and Experimental Physics (ITEP), Moscow, Russia
- ¹⁰⁰ National Research Nuclear University MEPhI, Moscow, Russia
- ¹⁰¹ D.V. Skobeltsyn Institute of Nuclear Physics, M.V. Lomonosov Moscow State University, Moscow, Russia
- ¹⁰² Fakultät für Physik, Ludwig-Maximilians-Universität München, München, Germany
- ¹⁰³ Max-Planck-Institut für Physik (Werner-Heisenberg-Institut), München, Germany
- ¹⁰⁴ Nagasaki Institute of Applied Science, Nagasaki, Japan
- ¹⁰⁵ Graduate School of Science and Kobayashi-Maskawa Institute, Nagoya University, Nagoya, Japan
- ¹⁰⁶ ^(a) INFN Sezione di Napoli; ^(b) Dipartimento di Fisica, Università di Napoli, Napoli, Italy
- ¹⁰⁷ Department of Physics and Astronomy, University of New Mexico, Albuquerque NM, United States
- ¹⁰⁸ Institute for Mathematics, Astrophysics and Particle Physics, Radboud University Nijmegen/Nikhef, Nijmegen, Netherlands
- ¹⁰⁹ Nikhef National Institute for Subatomic Physics and University of Amsterdam, Amsterdam, Netherlands
- ¹¹⁰ Department of Physics, Northern Illinois University, DeKalb IL, United States
- ¹¹¹ Budker Institute of Nuclear Physics, SB RAS, Novosibirsk, Russia
- ¹¹² Department of Physics, New York University, New York NY, United States
- ¹¹³ Ohio State University, Columbus OH, United States
- ¹¹⁴ Faculty of Science, Okayama University, Okayama, Japan
- ¹¹⁵ Homer L. Dodge Department of Physics and Astronomy, University of Oklahoma, Norman OK, United States
- ¹¹⁶ Department of Physics, Oklahoma State University, Stillwater OK, United States
- ¹¹⁷ Palacký University, RCPTM, Olomouc, Czech Republic
- ¹¹⁸ Center for High Energy Physics, University of Oregon, Eugene OR, United States
- ¹¹⁹ LAL, Univ. Paris-Sud, CNRS/IN2P3, Université Paris-Saclay, Orsay, France
- ¹²⁰ Graduate School of Science, Osaka University, Osaka, Japan
- ¹²¹ Department of Physics, University of Oslo, Oslo, Norway
- ¹²² Department of Physics, Oxford University, Oxford, United Kingdom
- ¹²³ ^(a) INFN Sezione di Pavia; ^(b) Dipartimento di Fisica, Università di Pavia, Pavia, Italy
- ¹²⁴ Department of Physics, University of Pennsylvania, Philadelphia PA, United States
- ¹²⁵ National Research Centre "Kurchatov Institute" B.P. Konstantinov Petersburg Nuclear Physics Institute, St. Petersburg, Russia
- ¹²⁶ ^(a) INFN Sezione di Pisa; ^(b) Dipartimento di Fisica E. Fermi, Università di Pisa, Pisa, Italy
- ¹²⁷ Department of Physics and Astronomy, University of Pittsburgh, Pittsburgh PA, United States
- ¹²⁸ ^(a) Laboratório de Instrumentação e Física Experimental de Partículas – LIP, Lisboa; ^(b) Faculdade de Ciências, Universidade de Lisboa, Lisboa; ^(c) Department of Physics, University of Coimbra, Coimbra; ^(d) Centro de Física Nuclear da Universidade de Lisboa, Lisboa; ^(e) Departamento de Física, Universidade do Minho, Braga; ^(f) Departamento de Física Teórica y del Cosmos and CAFPE, Universidad de Granada, Granada (Spain); ^(g) Dep Física and CEFITEC of Faculdade de Ciências e Tecnologia, Universidade Nova de Lisboa, Caparica, Portugal
- ¹²⁹ Institute of Physics, Academy of Sciences of the Czech Republic, Praha, Czech Republic
- ¹³⁰ Czech Technical University in Prague, Praha, Czech Republic
- ¹³¹ Faculty of Mathematics and Physics, Charles University in Prague, Praha, Czech Republic
- ¹³² State Research Center Institute for High Energy Physics (Protvino), NRC KI, Russia
- ¹³³ Particle Physics Department, Rutherford Appleton Laboratory, Didcot, United Kingdom
- ¹³⁴ ^(a) INFN Sezione di Roma; ^(b) Dipartimento di Fisica, Sapienza Università di Roma, Roma, Italy
- ¹³⁵ ^(a) INFN Sezione di Roma Tor Vergata; ^(b) Dipartimento di Fisica, Università di Roma Tor Vergata, Roma, Italy
- ¹³⁶ ^(a) INFN Sezione di Roma Tre; ^(b) Dipartimento di Matematica e Fisica, Università Roma Tre, Roma, Italy
- ¹³⁷ ^(a) Faculté des Sciences Ain Chock, Réseau Universitaire de Physique des Hautes Energies – Université Hassan II, Casablanca; ^(b) Centre National de l'Energie des Sciences Techniques Nucleaires, Rabat; ^(c) Faculté des Sciences Semlalia, Université Cadi Ayyad, LPHEA-Marrakech; ^(d) Faculté des Sciences, Université Mohamed Premier and LPTPM, Oujda; ^(e) Faculté des sciences, Université Mohammed V, Rabat, Morocco
- ¹³⁸ DSM/IRFU (Institut de Recherches sur les Lois Fondamentales de l'Univers), CEA Saclay (Commissariat à l'Energie Atomique et aux Energies Alternatives), Gif-sur-Yvette, France
- ¹³⁹ Santa Cruz Institute for Particle Physics, University of California Santa Cruz, Santa Cruz CA, United States
- ¹⁴⁰ Department of Physics, University of Washington, Seattle WA, United States
- ¹⁴¹ Department of Physics and Astronomy, University of Sheffield, Sheffield, United Kingdom
- ¹⁴² Department of Physics, Shinshu University, Nagano, Japan
- ¹⁴³ Fachbereich Physik, Universität Siegen, Siegen, Germany
- ¹⁴⁴ Department of Physics, Simon Fraser University, Burnaby BC, Canada
- ¹⁴⁵ SLAC National Accelerator Laboratory, Stanford CA, United States
- ¹⁴⁶ ^(a) Faculty of Mathematics, Physics & Informatics, Comenius University, Bratislava; ^(b) Department of Subnuclear Physics, Institute of Experimental Physics of the Slovak Academy of Sciences, Kosice, Slovak Republic
- ¹⁴⁷ ^(a) Department of Physics, University of Cape Town, Cape Town; ^(b) Department of Physics, University of Johannesburg, Johannesburg; ^(c) School of Physics, University of the Witwatersrand, Johannesburg, South Africa
- ¹⁴⁸ ^(a) Department of Physics, Stockholm University; ^(b) The Oskar Klein Centre, Stockholm, Sweden
- ¹⁴⁹ Physics Department, Royal Institute of Technology, Stockholm, Sweden
- ¹⁵⁰ Departments of Physics & Astronomy and Chemistry, Stony Brook University, Stony Brook NY, United States
- ¹⁵¹ Department of Physics and Astronomy, University of Sussex, Brighton, United Kingdom
- ¹⁵² School of Physics, University of Sydney, Sydney, Australia
- ¹⁵³ Institute of Physics, Academia Sinica, Taipei, Taiwan
- ¹⁵⁴ Department of Physics, Technion: Israel Institute of Technology, Haifa, Israel
- ¹⁵⁵ Raymond and Beverly Sackler School of Physics and Astronomy, Tel Aviv University, Tel Aviv, Israel
- ¹⁵⁶ Department of Physics, Aristotle University of Thessaloniki, Thessaloniki, Greece
- ¹⁵⁷ International Center for Elementary Particle Physics and Department of Physics, The University of Tokyo, Tokyo, Japan
- ¹⁵⁸ Graduate School of Science and Technology, Tokyo Metropolitan University, Tokyo, Japan
- ¹⁵⁹ Department of Physics, Tokyo Institute of Technology, Tokyo, Japan

- ¹⁶⁰ Tomsk State University, Tomsk, Russia
¹⁶¹ Department of Physics, University of Toronto, Toronto ON, Canada
¹⁶² ^(a) INFN-TIFPA; ^(b) University of Trento, Trento, Italy
¹⁶³ ^(a) TRIUMF, Vancouver BC; ^(b) Department of Physics and Astronomy, York University, Toronto ON, Canada
¹⁶⁴ Faculty of Pure and Applied Sciences, and Center for Integrated Research in Fundamental Science and Engineering, University of Tsukuba, Tsukuba, Japan
¹⁶⁵ Department of Physics and Astronomy, Tufts University, Medford MA, United States
¹⁶⁶ Department of Physics and Astronomy, University of California Irvine, Irvine CA, United States
¹⁶⁷ ^(a) INFN Gruppo Collegato di Udine, Sezione di Trieste, Udine; ^(b) ICTP, Trieste; ^(c) Dipartimento di Chimica, Fisica e Ambiente, Università di Udine, Udine, Italy
¹⁶⁸ Department of Physics and Astronomy, University of Uppsala, Uppsala, Sweden
¹⁶⁹ Department of Physics, University of Illinois, Urbana IL, United States
¹⁷⁰ Instituto de Física Corpuscular (IFIC) and Departamento de Física Atómica, Molecular y Nuclear and Departamento de Ingeniería Electrónica and Instituto de Microelectrónica de Barcelona (IMB-CNM), University of Valencia and CSIC, Valencia, Spain
¹⁷¹ Department of Physics, University of British Columbia, Vancouver BC, Canada
¹⁷² Department of Physics and Astronomy, University of Victoria, Victoria BC, Canada
¹⁷³ Department of Physics, University of Warwick, Coventry, United Kingdom
¹⁷⁴ Waseda University, Tokyo, Japan
¹⁷⁵ Department of Particle Physics, The Weizmann Institute of Science, Rehovot, Israel
¹⁷⁶ Department of Physics, University of Wisconsin, Madison WI, United States
¹⁷⁷ Fakultät für Physik und Astronomie, Julius-Maximilians-Universität, Würzburg, Germany
¹⁷⁸ Fakultät für Mathematik und Naturwissenschaften, Fachgruppe Physik, Bergische Universität Wuppertal, Wuppertal, Germany
¹⁷⁹ Department of Physics, Yale University, New Haven CT, United States
¹⁸⁰ Yerevan Physics Institute, Yerevan, Armenia
¹⁸¹ Centre de Calcul de l'Institut National de Physique Nucléaire et de Physique des Particules (IN2P3), Villeurbanne, France

- ^a Also at Department of Physics, King's College London, London, United Kingdom.
^b Also at Institute of Physics, Azerbaijan Academy of Sciences, Baku, Azerbaijan.
^c Also at Novosibirsk State University, Novosibirsk, Russia.
^d Also at TRIUMF, Vancouver BC, Canada.
^e Also at Department of Physics & Astronomy, University of Louisville, Louisville, KY, United States of America.
^f Also at Physics Department, An-Najah National University, Nablus, Palestine.
^g Also at Department of Physics, California State University, Fresno CA, United States of America.
^h Also at Department of Physics, University of Fribourg, Fribourg, Switzerland.
ⁱ Also at Departament de Física de la Universitat Autònoma de Barcelona, Barcelona, Spain.
^j Also at Departamento de Física e Astronomia, Faculdade de Ciências, Universidade do Porto, Portugal.
^k Also at Tomsk State University, Tomsk, Russia, Russia.
^l Also at Università di Napoli Parthenope, Napoli, Italy.
^m Also at Institute of Particle Physics (IPP), Canada.
ⁿ Also at Horia Hulubei National Institute of Physics and Nuclear Engineering, Bucharest, Romania.
^o Also at Department of Physics, St. Petersburg State Polytechnical University, St. Petersburg, Russia.
^p Also at Department of Physics, The University of Michigan, Ann Arbor MI, United States of America.
^q Also at Centre for High Performance Computing, CSIR Campus, Rosebank, Cape Town, South Africa.
^r Also at Louisiana Tech University, Ruston LA, United States of America.
^s Also at Institutio Catalana de Recerca i Estudis Avançats, ICREA, Barcelona, Spain.
^t Also at Graduate School of Science, Osaka University, Osaka, Japan.
^u Also at Institute for Mathematics, Astrophysics and Particle Physics, Radboud University Nijmegen/Nikhef, Nijmegen, Netherlands.
^v Also at Department of Physics, The University of Texas at Austin, Austin TX, United States of America.
^w Also at Institute of Theoretical Physics, Ilia State University, Tbilisi, Georgia.
^x Also at CERN, Geneva, Switzerland.
^y Also at Georgian Technical University (GTU), Tbilisi, Georgia.
^z Also at Ochadai Academic Production, Ochanomizu University, Tokyo, Japan.
^{aa} Also at Manhattan College, New York NY, United States of America.
^{ab} Also at Academia Sinica Grid Computing, Institute of Physics, Academia Sinica, Taipei, Taiwan.
^{ac} Also at School of Physics, Shandong University, Shandong, China.
^{ad} Also at Departamento de Física Teórica y del Cosmos and CAFPE, Universidad de Granada, Granada (Spain), Portugal.
^{ae} Also at Department of Physics, California State University, Sacramento CA, United States of America.
^{af} Also at Moscow Institute of Physics and Technology State University, Dolgoprudny, Russia.
^{ag} Also at Departement de Physique Nucléaire et Corpusculaire, Université de Genève, Geneva, Switzerland.
^{ah} Also at Eotvos Lorand University, Budapest, Hungary.
^{ai} Also at Departments of Physics & Astronomy and Chemistry, Stony Brook University, Stony Brook NY, United States of America.
^{aj} Also at International School for Advanced Studies (SISSA), Trieste, Italy.
^{ak} Also at Department of Physics and Astronomy, University of South Carolina, Columbia SC, United States of America.
^{al} Also at Institut de Física d'Altes Energies (IFAE), The Barcelona Institute of Science and Technology, Barcelona, Spain.
^{am} Also at School of Physics, Sun Yat-sen University, Guangzhou, China.
^{an} Also at Institute for Nuclear Research and Nuclear Energy (INRNE) of the Bulgarian Academy of Sciences, Sofia, Bulgaria.
^{ao} Also at Faculty of Physics, M.V. Lomonosov Moscow State University, Moscow, Russia.
^{ap} Also at Institute of Physics, Academia Sinica, Taipei, Taiwan.
^{aq} Also at National Research Nuclear University MEPhI, Moscow, Russia.
^{ar} Also at Department of Physics, Stanford University, Stanford CA, United States of America.
^{as} Also at Institute for Particle and Nuclear Physics, Wigner Research Centre for Physics, Budapest, Hungary.
^{at} Also at Giresun University, Faculty of Engineering, Turkey.
^{au} Also at Flensburg University of Applied Sciences, Flensburg, Germany.
^{av} Also at CPPM, Aix-Marseille Université and CNRS/IN2P3, Marseille, France.
^{aw} Also at University of Malaya, Department of Physics, Kuala Lumpur, Malaysia.
^{ax} Also at LAL, Univ. Paris-Sud, CNRS/IN2P3, Université Paris-Saclay, Orsay, France.
^{ay} Also affiliated with PKU-CHEP.
^{*} Deceased.